III Results and Discussion

Although a number of studies have evidently shown that dynamin is required for endocytosis, only recently has first evidence been obtained that dynamin isoforms may also function in exocytosis. The initial studies on binding of dynamin II to the trans-Golgi network of hepatoma cells (Maier et al., 1996) have been extended by the finding that addition of dynamin-specific antibodies to an *in vitro* system of vesicle biogenesis inhibited the formation of exocytic and of clathrin-coated vesicles at the TGN (Jones et al., 1998). The report implied that dynamin II participated in the formation of post-Golgi vesicles. However, there are also contradictory reports that deny any effect on constitutive transport of newly sythesized TfnR to the plasma membrane or clathrin-mediated transport of cathepsin D to the lysosome using overexpression of dyn-2 (K44A) mutant (Altschuler et al., 1998). Since dynamin II localizes to the TGN (Maier et al., 1996), we assume that dynamin may function at the Golgi apparatus. To find more evidences to support this view and further understand the mechanism(s) by which dynamin II functions, we cloned dynamin II domains and studied their structures. On this basis, function of dynamin II domains in vesicle budding from the TGN *in vitro* and their impacts on secretion of glycoproteins in living cells were analyzed. Moreover, localization of dynamin II domains and of the endogenous dynamin II in mammalian cells was studied. The findings will be discussed in regard to putative mechanism(s) by which dynamin II may support vesicle biogenesis at the Golgi.

3.1 Cloning of dynamin II domains

3.1.1 PCR amplification of DNAs coding for pleckstrin-homology domain (PHD), proline-rich domain (PRD) and the C-terminal half domain (PCP) of dynamin II

To study the function of individual domain of dynamin II independent of the GTPase domain, the PHD, the PRD and the C-terminal half of dynamin II (PCP) were individually cloned on the basis of a dynamin II cDNA obtained from Dr.C. Diatloff-Zito {Diatloff, Gordon, et al. 1995 990 /id}. The cDNA codes for the bb spliced variant {Cao, Garcia, et al. 1998 716 /id}. Specific primers (Figure 10 A) were designed and optimized by computer, with the program WINSTAR, Primer-select, to reduce potential hairpin structures and primer dimerization. The 5´ PCR primers were extended by a Bgl II

restriction site and the 3´ PCR primers by an EcoR I site. Individual primer pairs were used to amplify PHD and PRD fragments, whereas PHD primer 1 and PRD primer 2 were used to generate the PCP (500-870) which includes PHD, coiled-coil domain (CCD) and PRD. PCR amplification resulted in the formation of three DNA fragments with the expected lengths (Figure 10 B). No other PCR products were observed.

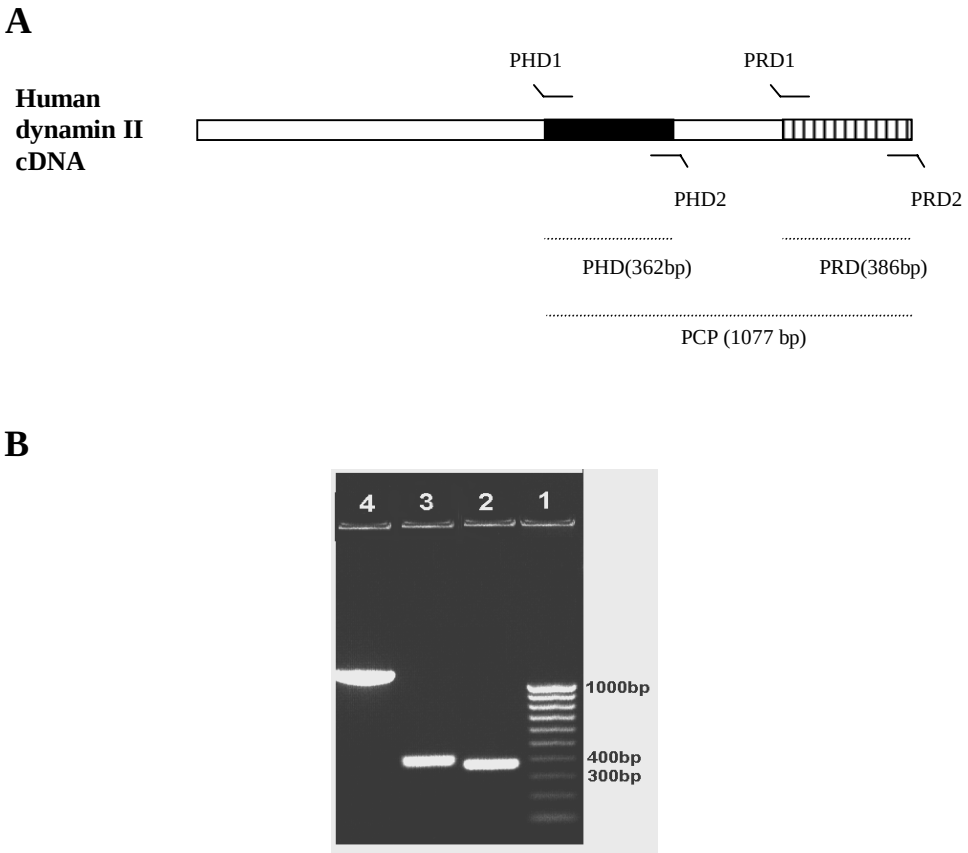

Figure 10. Amplification of three dynamin II domains. Specific PCR primers (A) were designed by PC program WINSTAR Primer-select based on the sequence of human dynamin II cDNA. The PCR products were analyzed by EB-agarose gel electophoresis (B). 1: DNA molecular weight ladder. 2: PHD fragment (362bp). 3: PRD fragment (386bp). 4: PCP fragment (1077bp)

3.1.2 Cloning and DNA sequencing of PCR products

Ligation of three PCR fragments into the expression vector pTrcHis2C resulted in three recombinant plsmids, ptrc-PHD, pTrc-PRD and pTrc-PCP (Figure 6 A). Purified plasmids were obtained from transformed *E.coli* Top-10. The successful ligation was confirmed by

==========

analyzing the size of three fragments with restriction enzyme digestion and EB-agarose gel electrophoresis (Figure 6 B). Sequencing the fragments proved their identity with the corresponding regions of the template cDNA. (see Appendix A and Appendix F for dynamin II domain sequences).

3.1.3 Subcloning of dynamin II domains into prokaryotic expression vectors

In order to obtain sufficient amount of dynamin II domain proteins for *in vitro* study, we used the expression vector pTrcHis2 (Invitrogen) and pET-30a(+) (Novagen). Both of these two vectors were designed for efficient expression of foreign proteins (compare 2.2.2.1). Three DNA fragments cloned in pTrcHis2C vector (Figure 6 A) were fused with a sequence coding for the *myc* epitope that can be used to identify the expressed proteins using the anti-*myc* antibody. In addition, a $(His)_6$ sequence was tagged at the C-terminus to purify the recombinant dynamin II domain proteins PHD-his, PRD-his and PCP-his by using the Ni-NTA-agarose chromatography.

The pET-30a(+) vector provides two tags, $(His)_6$ tag and S-peptide tag, both of which are fused to N-terminus of the recombinant proteins. Therefore, we could purify recombinant proteins by using either the Ni-NTA-agarose or the S-protein agarose chromatography. The S-protein immobilized on agarose forms a tight complex with S-peptide and reconstitutes the stable RNase A structure (compare 3.2.7). Binding of S-peptide tagged proteins to the S-agarose is resistant to stringent wash conditions, such as 2 M urea containing buffer. The three dynamin domain proteins expressed with pET-30a(+) constructs were designated as his-s-PHD, his-s-PRD and his-s-PCP, respectively (Figure 7).

The full amino acid sequcence of dynamin II domains expressed in *E.coli* were listed in Appendix F.

3.1.4 Subcloning of dynamin II domains into mammalian expression vectors

To study celluar localization, dynamin II domains were fused with EGFP using the pEGFP-C1 vector (Clontech, Figure 8). The EGFP was fused to the N-terminus of fusion proteins and allowed us to monitor the expression and the localization of dynamin II domains in mammalian cells by immunofluorescence microscopy.

In order to study functions of dynamin II domains in living cells, permanent cell lines that express dynamin II domains were established. To minimize possible lethal effect of dynamin II domains, we used a tetracycline regulated expression system (Tet-on, Invitrogen). The dynamin II domains tagged with EGFP were subcloned into vector

pcDNA4/TO/*myc*-His (Figure 9), which contained a human CMV promoter regulated by two tetracycline operator 2 (TetO2) sites. As a result, the expression of domain proteins was suppressed by the Tet repressor which was expressed from pcDNA6/TR plasmid after being co-transfected. In the absence of tetracycline, expression of gene of interest was repressed by the binding of Tet repressor homodimers to the TetO2 sequences. Addition of tetracycline to the cells blocked Tet repressor derepress the hybrid CMV/TetO2 promoter in pcDNA4/TO/*myc*-His and then the downstream gene was expressed.

3.2 Expression and purification of dynamin II domains

3.2.1 Expression of dynamin II domains with a C-terminal $(His)_6$ tag

Competent *E. coli* Top-10 bacterial cells were transformed with recombinant plasmids pTrc-PHD, pTrc-PRD or pTrc-PCP and cultivated to a density of $OD_{600} \approx 0.5$ in LB medium. Expression of dynamin II domains was induced by addition of 1 mM IPTG for 3 h at 37°C. Analysis of the lysed bacterial proteins by SDS-PAGE showed a prominent band of PHD-his with an apparent molecular weight of 22 kD (Figure 11). The bands representing PRD-his and PCP-his were not viewed by Coomassie brilliant blue (CBB) staining, suggesting a low expression level and/or co-migration of the two proteins with bacterial protein bands. To demonstrate their expression, proteins were transferred to the nitrocellulose membrane for immunodetection. Since all three recombinant proteins were tagged with a *myc* epitope at the C-terminal end, they could be detected with an antibody to the *myc* epitope. Incubation with HRP-conjugated secondary antibody to mouse IgG and Phototope detection showed three specific bands corresponding to molecular weights of 22, 25 and 48 kD, respectively (Figure 12). Immuno-detection proved that the PRD-his and PCP-his were expressed but the expression levels were too low to be recognized by CBB staining. Detection of C-terminal tags of recombinant proteins by the anti-*myc* antibody also confirmed expression of the correct reading frame. Gel scans showed that PHD-his protein was expressed to 15-20 % of total cell proteins, while PRD-his and PCP-his amounted to less than 5 %.

In order to increase the expression level of PRD-his and PCP-his, we tested different bacterial hosts and growth media. Among different hosts tested, expression levels of PRD-his and PCP-his in *E.coli* BL21(DE3) were 2 to 3 fold higher than the average, whereas different media (such as LB, SOB and M9) had no impact on expression levels.

==========

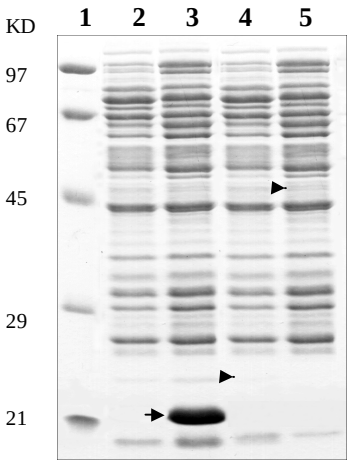

Figure 11. Expression of dynamin II domains using pTrcHis2C vector-based constructs. Expression of PHD-his is recognized by Coomassie blue staining (arrow), whereas expressin of PRD-his and PCP-his are too low to form a distinct band,. Their positions are indicated by arrow heads.

1. Protein MW marker
2. Mock control
3. PHD-his expressing cell lysate
4. PRD-his expressing cell lysate
5. PCP-his expressing cell lysate

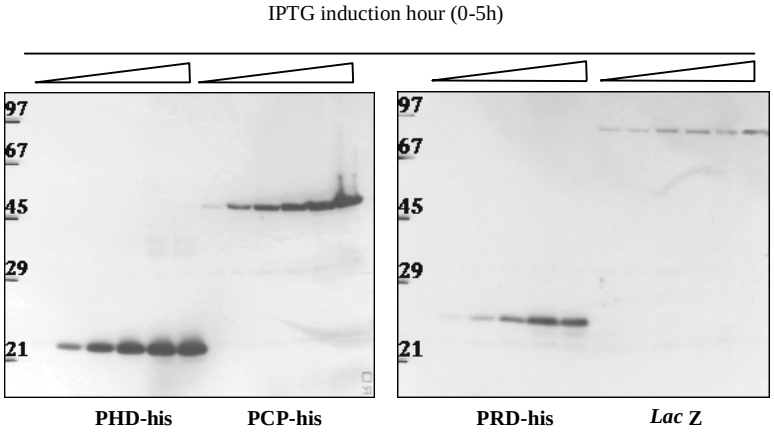

Figure 12. Analysis of *myc*-tagged dynamin II domains expressed using pTrcHis2C vectors-based constructs. Cultures of transformed *E.coli* were induced with 1mM IPTG for 0, 1, 2, 3, 4 and 5 h at 37°C. *E.coli* lysates were analyzed by SDS-PAGE and Western blotting using an anti-*myc* antibody. *E.coli* transformed with a pTrcHis2-*Lac* Z plasmid was used as a positive control (Invitrogen). Note: PHD-his sample loaded was ¼ of the other three samples)

==========

The kinetic analysis of induction showed that the expression was low before 1 h and reached maximum levels at 3-5 h after IPTG addition (Figure 12).

3.2.2 Purification of PHD-his protein

The pTrcHis2 vector, which codes for a C-terminal $(His)_6$ tag, allowed a simple purification of the recombinant protein by immobilized metal affinity chromatography (IMAC) using a nickel-charged agarose resin, such as Ni-NTA agarose resin (Qiagen) or ProBond^{TM} Resin (Invitrogen). Proteins bound to resin could be eluted either at low pH condition or by competition with imidazole or histidine.

To purify PHD-his, the bacterial lysate was loaded onto a Ni-NTA agarose column. After throughly washing with PBS buffer containing 1 M NaCl and 50 mM imidazole, the recombinant protein was eluted with PBS containing 250 mM imidazole. PHD-his was obtained in a purity of about 90 % (Figure 13 A and Figure 14 lane 2). Further purification to 96 % was achieved by chromatography on a Superdex 75 column (Figure 14 lane 3). The purified PHD-his was stored at -80°C in aliquots at a concentration of 1.5mg/ml.

3.2.3 Purification of PRD-his and PCP-his proteins

While the PHD-his was easily purified by Ni-NTA agarose chromatography, binding of PRD-his and PCP-his to Ni-NTA agarose was weak and both proteins were eluted together with bacterial proteins by imidazole ranging between 20 and 100 mM (Figure 13 B and C). The purity of both proteins amounted to less than 10% using Ni-NTA-agarose chromatography under native condition. Also, addition of 8 M urea to the buffers did not improve the separation, suggesting that these two proteins have low binding affinities to Ni-NTA agarose. Also, chromatography on Superdex 75 and Mono-S column (Phamacia) did not remove contaminating proteins.

Three reasons may be responsible for low expression and poor purification of PRD-his and PCP-his:

(1). The recombinant PRD and PCP domain proteins that may interact with *E.coli* proteins interfered with cellular functions and became poisonous to host cells. This toxicity may suppress protein synthesis which also could happen in uninduced cells, since a basal level of expression before induction was observed (Figure 12). To overcome these drawbacks, an expression system should have a more stringent control.

==========

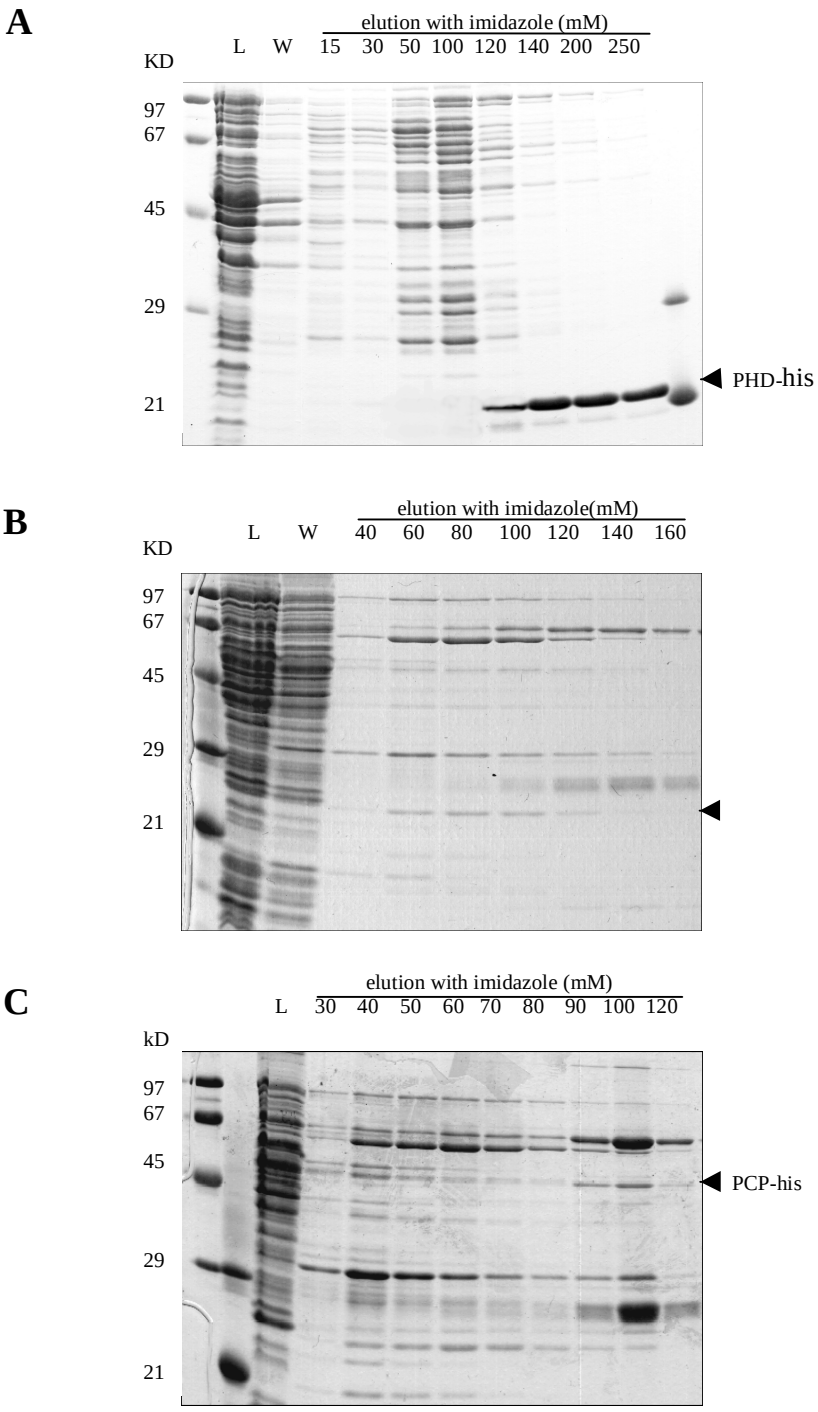

Figure 13. Purification of dynamin II domain PHD-his, PRD-his and PCP-his with Ni-NTA-agarose chromatography. pTrc-PHD transformed *E.coli* Top-10 cells (A), pTrc-PRD or pTrc-PCP transformed *E.coli* BL21(DE3) cells (B & C) were grown in LB medium and induced with 1mM IPTG for 3 h. Bacteria were harvested by centrifugation and lysed by sonication. Lysates (L) were incubated with Ni-NTA-agarose at 4°C for 2 h. Thereafter, the agarose was washed (W). The dynamin II domain proteins were eluted from the Ni-NTA-agarose column with increasing concentrations of imidazole as indicated in the figures. PHD-his could be purified in sufficient amount, whereas PRD-his and PCP-his were not separated from bacterial proteins

==========

(2). The *myc* epitope sequence and $(His)_6$ tag at C-terminal end of recombinant proteins may interact with the domain proteins and therefore resulted in a reduced binding affinity to Ni-NTA agarose. Due to this, N-terminally tagged constructs were used for further studies.

(3). Unspecific interactions between PRD-his or PCP-his and bacterial proteins, as well as strong binding of *E.coli* proteins to Ni-NTA agarose, were observed. Both effects may hinder separation in NTA agarose and Superdex 75 column chromatography.

To overcome these difficulties, we chose a T7 expression system in which the target gene was set under control of strong bacteriophage T7 transcription and translation signals. Expression of recombinant proteins was induced by synthesis of T7 RNA polymerase in the host cell (Studier et al., 1990). An important benefit of the vector pET-30a(+) was its ability to maintain target genes transcriptionally silent in the uninduced state (Rosenberg et al., 1987). Target genes were initially cloned using hosts *E.coli* HM174 which did not contain the T7 RNA polymerase gene, thus eliminating plasmid instability that occurred due to the potential production of toxic proteins. Once established in a non-expression host, plasmids were transferred into the expression host BL21(DE3)pLysS which contained a chromosomal copy of the T7 RNA polymerase gene under *lacUV5* control. Expression of recombinant protein could be induced by addition of IPTG. The presence of pLysS increased the tolerance of DE3 lysogens for plasmids with toxic inserts. Therefore, unstable plasmids became stable and plasmids that would not otherwise be established could be maintained and expressed (Studier, 1991).

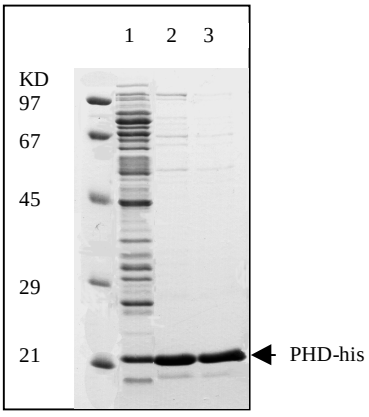

Figure 14. Purification of PHD-his. *E.coli.* Top-10 expressed PHD-his (lane 1) was purified by Ni-NTA-agarose chromatography (lane 2) and Superdex 75 chromatography (lane 3). Samples were analyzed by SDS-PAGE and Coomassie blue staining.

==========

3.2.4 Expression of dynamin II domains with an N-terminal $(His)_6$ tag

Plasmids pET30a(+)-PHD, pET30a(+)-PRD or pET30a(+)-PCP were transformed individually into *E. coli* BL21(DE3)pLysS. Protein expression was induced by addition of 0.4 mM IPTG in modified M9 medium (M9E). After 3-5 h incubation, all three dynamin II domain proteins were expressed at different levels (Figure 15 lane 2 & 3, Figure 16). Expression of his-s-PHD was higher (10-15 %) than that of other two domains amounting to 3-5% of total cell protein. Highest expression was observed 4 h after induction. We tested the effect of several media on expression and found that the composition of the media apparently affected the expression levels. LB medium or M9 alone were not sufficient to promote maximum expression. However, supplement with $MgSO_4$ and glucose apparently stimulated expression; therefore, we optimized the M9 medium by addition of 0.5-2% D-(+)glucose, 0.2% $MgSO_4$ and 0.01% $CaCl_2$ (for the composition of M9E see 2.1.7). M9E medium was used for further expression of all three proteins.

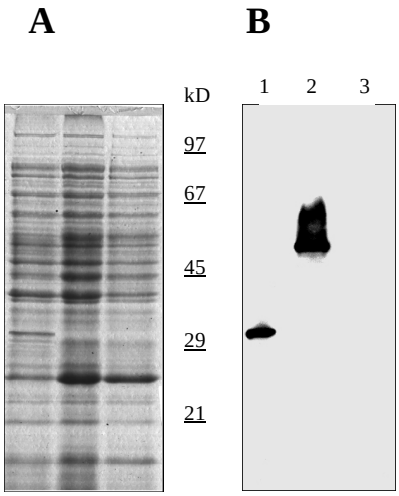

Figure 15. Expression of his-s-PRD and his-s-PCP. *E.coli* strains BL21(DE3)pLysS transformed with recombinant plasmids pTrc-PRD and pTrc-PCP were induced with IPTG at 37°C for 3 h. Lysates were loaded on SDS-PAGE and analyzed by Coomassie blue stainning (A) and Western blotting using an anti-dynamin II antibody (B).

1: his-s-PRD cell lysate

2: his-s-PCP cell lysate

3: lysate of *E. coli* tranformed with pTrcHis2C (mock control).

==========

3.2.5 Purification of his-s-PHD

$(His)_6$ and S-peptide tagged his-s-PHD was bound to Ni-NTA agarose and eluted with 200 mM imidazole. The high affinity binding resulted in a separation from most bacterial proteins. To remove remaining contaminating proteins, chromatography on a Superdex 75 column was applied. The main protein peak of his-s-PHD showed a purity of about 95% (Figure 16 A).

3.2.6 Purification of his-s-PRD

Purification of his-s-PRD was similar to that of his-s-PHD described above. We observed a higher binding affinity of his-s-PRD for Ni-NTA-agarose in comparison to PRD-his. Since his-s-PRD bound as efficient as his-s-PHD, stronger wash conditions such as PBS containing 0.5 M NaCl, 50 mM imidazole and 10 mM β-ME were applied that removed most contaminating proteins from Ni-NTA agarose. After a second purification step by Superdex 75 column chromatography (Figure 17), the purity of his-s-PRD was increased to 94 % (Figure 16 B). Because of the relatively low expression, the recombinant protein was prepared from 20 liter fermentation and finally 20 mg of purified his-s-PRD was obtained. For simplicity, his-s-PRD was designated PRD in the following experiments.

3.2.7 Purification of his-s-PCP

Transferring the $(His)_6$ tag from C-terminal to N-terminal end of PCP did not increase its binding affinity to Ni-NTA agarose. his-s-PCP binds to Ni-NTA agarose as weakly as PCP-his and was eluted already by the washing buffer containing 50 mM imidazole which was the lowest concentration required for removing the major contaminating *E.coli* proteins. Since the addition of urea did not improve binding, we had to use the S-peptide tag to isolate the his-s-PCP.

The S-tag (Novagen) is a protein tagging system based on the interaction of the N-terminal peptide of RNase A (the S-tag peptide) with the remaining 104 amino acid S-protein (Kim and Raines, 1993). The interaction between S-Tag and S-protein is very specific and strong ($K_d=10^{-9}$ M). In addition, the S-tag is easily soluble in water due to its composition (7 charged polar, 3 uncharged polar, and 5 nonpolar residues). It possesses little secondary structure and a low net charge at neutral pH. The S-tag is therefore unlikely to interfere with the proper folding or function of a fusion protein.

his-s-PCP was bound to S-protein agarose in the presence of 2 M urea to reduce unspecific interactions. After removing contaminating proteins by throughly washing, the his-s-PCP

==========

was eluted from the S-proteins agarose with 3 M $MgCl_2$, which resulted in the purity of 60 %. Chromatography on a Superdex 75 column further increased the purity to 92 % (Figure 16 C).

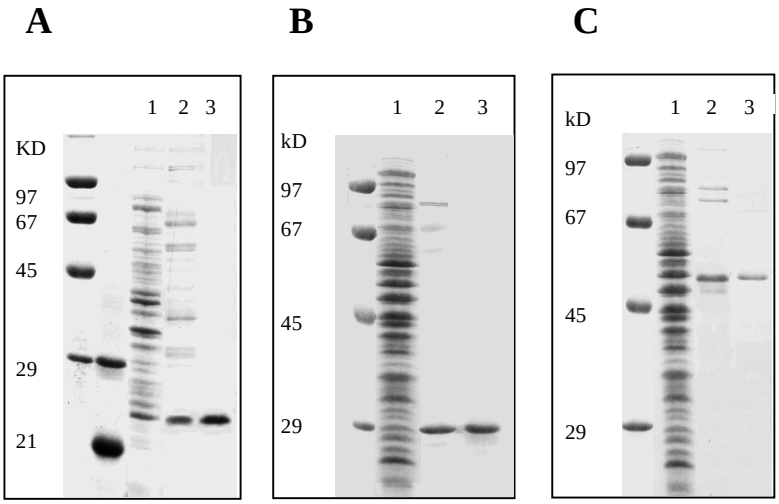

Figure 16. Purification of dynamin II domains his-s-PHD (A), his-s-PRD (B) and his-s-PCP (C). Domains were expressed in *E.coli* BL21(DE3)pLysS with pET-30a(+) constructs. Cell lysates (A, B and C, lanes 1) were purified by Ni-NTA agarose chromatography (A and B, lanes 2) or S-protein agarose chromatography (C, lane 2) and subsequently purified by Superdex 75 column chromatography (A, B and C, lanes 3).

To compare the expression results, the data of expression levels and purification of dynamin II domains in *E.coli* was summarized in Table 3.

Table 3. dynamin II domains expressed in *E.coli*

Domain	amino acids	MW(kD)	expression level(%)	final purity (%)
PHD-his	155	22	15-20	96
his-s-PHD	191	24	10-15	95
PRD-his	163	25	3-5	purification failed
his-s-PRD	199	30	5-8	94
PCP-his	401	47	3-5	purification failed
his-s-PCP	437	50	3-5	92

Note: PHD-his, PRD-his and PCP-his were expressed with pTrcHis2 constructs. His-s-PHD, his-s-PRD and his-s-PCP were expressed with pET-30a(+) constructs.

==========

The different purification levels suggested that several factors may affect the isolation of fusion proteins. These include the location of the tag sequence and the structural properties of proteins. The latter determines the interaction of recombinant proteins with the tag sequence or other bacterial proteins and then reduces the affinity of $(His)_6$ tag to Ni-NTA agarose. The high number of proline residues in the PRD inhibites proper folding (refer to Result 3.3) and may induce interaction with the C-terminal $(His)_6$ tag, reducing its ability to bind Ni-NTA agarose. In addition, the unfolded structure and the basic charge of PRD (pI=9.37) might also cause unspecific interactions with contaminating proteins. This may explain the failure for purification of the PRD-his protein. In the case of PCP purification, in addition to PRD, GED might also strongly influence the affinity of $(His)_6$ tag to Ni-NTA agarose because GED functions as a self-assembly domain in dynamin II molecules {Smirnova, Shurland, et al. 1999 684 /id}{Okamoto, Tripet, et al. 1999 705 /id} and may induce aggregation of recombinant protein. The successful purification of PHD with $(His)_6$ tag both at the C-terminus and at the N-terminus might be caused by highly ordered secondary structure of the domain which prevented interaction with other proteins (Dong et al., 2000b).

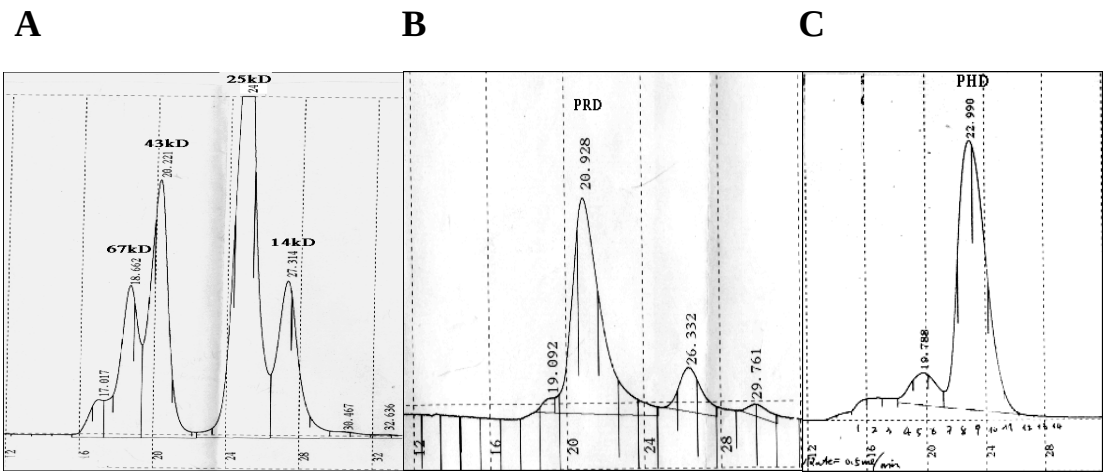

Figure 17. Chromatography of PHD-his (C) and his-s-PRD (B) on Superdex 75. After Ni-NTA-agarose chromtography, his-s-PRD (panel B) and PHD-his (panel C) were separated on Superdex 75 column in 20 mM sodium phosphate pH7.0, 50 mM NaCl, 0.2 mM DTT. Molecular weight standards (panel A) were run for comparison. BSA (67kD), ovalbumin (43kD), chymotrypsinogen A (25kD) and ribonuclease A (14kD).

==========

3.3 Conformation of dynamin II domains, PHD and PRD

Studies on functions of individual protein domains are based on the supposition that the expressed and purified domains adopt a conformation that is similar to the structure within the intact protein. Since the structure of dynamin II is not known, global features, e.g., spectroscopic properties, have to be used to characterize structures of isolated domains. Studies on the PHD can be correlated to the known crystal structure of the PHD of dynamin I consisting of about 13 % α-helix and 46 % β-structures (Timm et al., 1994a). Because of the extended sequence homology between PHDs of dynamin I and II (84 %), a high degree of structural similarity can be expected. A content of 20 % α-helix and 52 % β-structures was estimated according to Provencher and Glöckner (Goud et al., 1990) from the CD spectrum of PHD-his (Figure 18 A, curve 1). These data are in reasonable agreement with the above mentioned three-dimensional structure of the PHD of dynamin I (Timm et al., 1994a). The tertiary structure class determination, according to Venyaminov and Vassilenko (Venyaminov and Vassilenko, 1994), classified PHD-his as an α + β protein and agreed with the known crystal structure of the PHD from dynamin I. In accordance with a folded structure, the maximum of the tryptophan fluorescence was observed at about 332 nm (Figure 18 B, curve 1) as typical for a tryptophan in a hydrophobic environment. This indicates that the four tryptophan residues are predominantly buried in the hydrophobic core of the folded PHD. In 6 M guanidine hydrochloride, the maximum of emission shifted to about 350 nm as expected for an unfolded PHD-his when the tryptophan residues was exposed to the surrounding solvent (not shown).

Finally, gel chromatography on Superdex 75 supported the folded structure: PHD-his was eluted as a homogeneous peak for which an apparent molecular mass of about 25 kD (Figure 17 C) could be calculated using the globular marker proteins, chymotrypsinogen A and ovalbumin (Figure 17 A). This value was higher than the calculated molecular mass of 18.3 kD and indicated a significant deviation from the globular structure of a monomeric protein. Two effects may increase the apparent molecular mass of PHD-his: first, unstructured regions and flexible loop structures may exist that were identified by heteronuclear NMR spectroscopy of the PHD of dynamin I (Fushman et al., 1995); and second, the domain may dimerize in accordance with the PHD of dynamin I which crystallizes as a dimer (Timm et al., 1994b). Even if the structure in solution is predominantly monomeric, a fast monomer-dimer equilibrium may exist which could

result in the observed elution behavior (Uversky, 1993). Whether (i) the PHD may have an elongated shape or flexible loop(s), (ii) a monomer-dimer equilibrium may exist or (iii) both effects may influence the structure, can not be decided on the basis of the present data. Nevertheless, the results of the CD measurements and the elution behavior of PHD strongly support the structural similarity between the PHD of dynamin II and the reported structure of homologous PHD of dynamin I (Timm et al., 1994b).

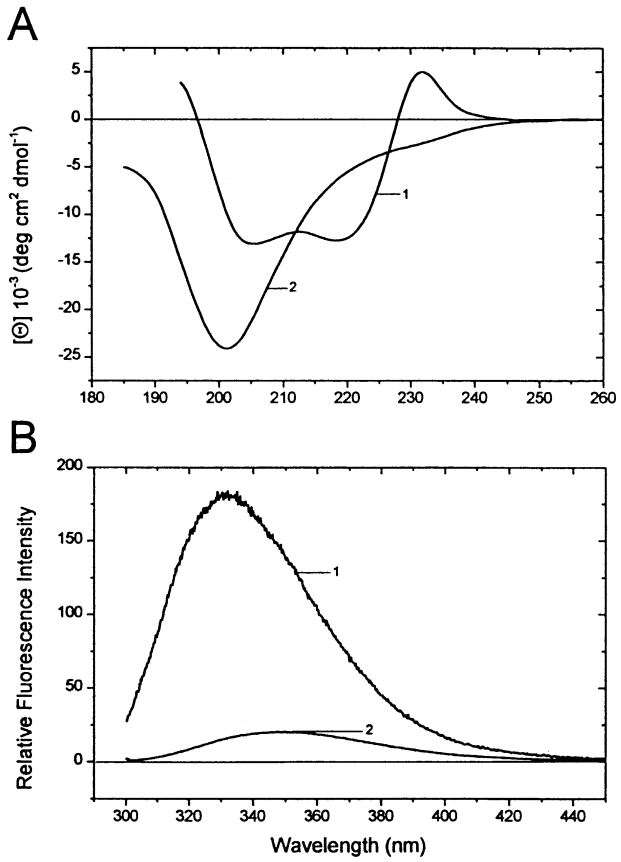

Figure 18. Circular dichroic (A) and fluoresence spectra (B) of PHD-his (1) and his-s-PRD (2) proteins measured in 20 mM sodium phosphate, pH7.0, 0.2 mM DTE, 50 mM NaCl as described in the Material and Methods, see 2.2.11.

No PRD structures, either from dynamin I or from dynamin II, are known. As a first approach, the sequence of PRD of dynamin II (his-s-PRD) was analyzed by a server program—PredictProtein (http://cubic.bioc.columbia.edu) published by Rost and Sander (Rost and Sander, 1993) (Rost, 1996). As expected for the high number of proline residues

==========

(see Figure 4), the program predicted a very low content of ordered secondary structure elements for the PRD: 13.1 % of the amino acids may form α-helices, while β-sheets are only 5.5 % and the majority of residues (81.4%) are in "other" structures representing neither α-helix nor β-structures (Appendix G). The major part of the PRD may therefore consist of unstructured loops or unfolded regions. Two extended helixes are attributed to the N-terminal peptide tags and only two short β-sheets composed of four-five amino acids are assigned to the PRD sequence (Appendix G).

The CD spectrum of his-s-PRD showed a dominant negative band at 200 nm (Figure 18 A, curve 2) similar to that of unfolded polypeptide chains. In fact, determination of the tertiary structure class from the CD spectrum, according to Venyaminov and Vassilenko (Venyaminov and Vassilenko, 1994), classified his-s-PRD as an unfolded protein. Nevertheless, there is a significant ellipticity at 222 nm. Taking the mean residue ellipticity at 222 nm as a measure of the α-helix content, $[\Theta]_{222}$ should amount to –1000 $deg \cdot cm^2 \cdot dmol^{-1}$ in case of the absence of α-helix or to –30 000 $deg \cdot cm^2 \cdot dmol^{-1}$ for a 100 % α-helix (Chen et al., 1974). The observed value of –4700 $deg \cdot cm^2 \cdot dmol^{-1}$ corresponds to a helix content of about 16 %. The latter can not be attributed to the poly-L-proline type II helix because this structure is characterized by a positive band near 228 nm (Bhatnagar and Gough, 1996) which is missing in the CD spectrum of PRD.

Further attempts to analyze the spectrum with the program CONTIN and sets of 16 (Provencher and Glöckner, 1981) or 20 reference proteins (Venyaminov et al., 1993) yielded excellent fits of the calculated spectra to the experimental spectrum yet, significantly different contents of secondary structure elements. With the set of 16 CD reference spectra, 22 % α-helix and 22 % β-sheets as well as 56 % of other structures were calculated. However, using the larger set of 20 reference proteins completed by three spectra of denatured proteins and one oligonucleotide spectrum (Venyaminov and Vassilenko, 1994) resulted in prediction of only 15 % α-helix, 12 % β-sheet and 73 % other structures. These values may fit better since including unfolded proteins in the reference set of CD spectra will improve the evaluation of the CD spectrum of an unfolded protein (Venyaminov and Vassilenko, 1994).

The maximum of the tryptophan fluorescence spectrum of his-s-PRD was located near 349 nm (Figure 18 B, curve 2), indicating a hydrophilic environment of the single tryptophan residue. A solvent accessibility of the tryptophan (see Appendix G) in an unfolded region

==========

of the protein confirmed the interpretation of the CD data. Altogether, CD and fluorescence spectra characterized his-s-PRD as a largely unfolded protein.

Gel exclusion chromatography on Superdex 75 demonstrated that his-s-PRD of a molecular mass of 20.8 kD behaved similarly to a globular protein of about 40 kD (Figure 17 B). This might indicate the formation of dimers but - considering the predicted secondary structure and the results of the CD measurements - the elution behavior most probably reflected the unfolded structure of his-s-PRD. Therefore, for the first time, the data provided experimental evidence for an unfolded and flexible structure of the PRD of dynamin II. The high flexibility of the polypeptide chain could support the formation of protein-protein contacts. Since an increasing number of unstructured proteins with distinct biological functions has been recognized, some of which are involved in molecular recognition and signaling (Wright and Dyson, 1999), the capacity of his-s-PRD to exert specific functions was tested by measuring its binding to membranes and proteins (see next).

3.4 The PRD of dynamin II interacts with SH3 domains of amphiphysin II and syndapin

The PRD of dynamin I has been known to bind to SH3 domains and mediates protein-protein interactions (Wigge and McMahon, 1998; Wigge et al., 1997). A fusion protein of PRD with GST was able to interact with amphiphysin I and II (Slepnev et al., 1998). Additional proteins, like clathrin and adaptins (David et al., 1996; Gonzalez and Jackle, 1997), were probably bound indirectly via their affinities for amphiphysins (Slepnev et al., 1998) (McMahon et al., 1997) (Ramjaun and McPherson, 1998). To test whether the PRD of dynamin II has similar protein binding properties, the PRD domain tagged with an S-peptide was immobilized to S-protein agarose and used for binding studies. Incubation of the *in vitro* expressed SH3 domain of amphiphysin II fused to GST demonstrated that the PRD specifically binds to the SH3 domain of amphiphysin II (Figure 19, lane 2). In comparison, PHD-his was unable to interact with the SH3 domain (Figure 19, lane 3), and his-s-PCP that contains the PHD and the GED, in addition to the PRD, was also able to bind the SH3 domain (Figure 19, lane 4). The binding of PRD to SH3 domain of amphiphysin I/II indicates similar binding sites for dynamin I and dynamin II. On the basis of this finding, it is tempting to speculate that both dynamins may function in clathrin-mediated endocytosis by interaction with amphiphysin I and amphiphysin II which have

==========

been located to clathrin-coated pits at the plasma membrane (Wigge and McMahon, 1998; McMahon et al., 1997; Simpson et al., 1999).

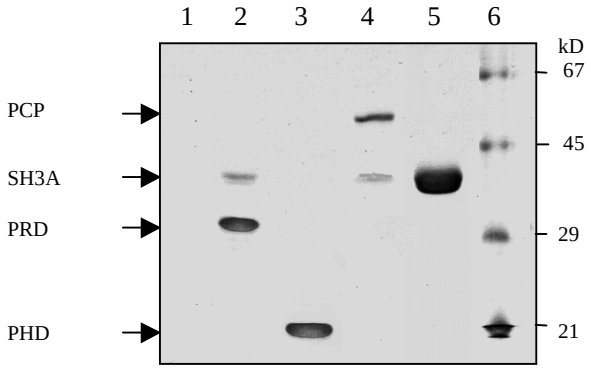

Figure 19. Binding of the SH3 domain of amphiphysin II to PRD and PCP. 5 µg SH3 domain fused to GST (SH3A) were incubated with S-protein agarose as a control (lane 1), with 2 µg PRD bound to S-protein agarose (lane 2), with 2 µg PHD attached to Ni-NTA agarose (lane 3) or with 1 µg PCP attached to S-protein agarose (lane 4). Proteins eluted with SDS-containing buffer were separated by SDS-PAGE and stained with Coomassie brilliant blue. 5 µg SH3 domain were run as a control (lane 5).

In addition, PRD binds to the SH3 domain of syndapin I, a newly identified cellular protein involved in vesicle trafficking and actin organization {Qualmann, Roos, et al. 1999 718 /id}{Qualmann & Kelly 2000 5196 /id}. We could demonstrated that recombinant SH3 domains of syndapin I and II specifically bound to the recombinant PRD (Figure 20, lane 4 and 5), whereas the P434L mutant of syndapin I containing a defective SH3 domain did not bind to PRD of dynamin II (Figure 20, lane 6). This demonstrated that the PRD of dynamin II is able to interact with SH3 domains. Binding specificities towards SH3 domains may be similar between PRDs of dynamin I and II, although the sequence homology is lower compared to other domains of dynamins (compare to Figure 2).

Additionally, the binding of SH3 domain was an important hint that the *in vitro* expressed PRD characterized by an “unfolded” structure maintains binding properties of native dynamin II and could, therefore, be used to study biological functions and protein binding partners.

==========

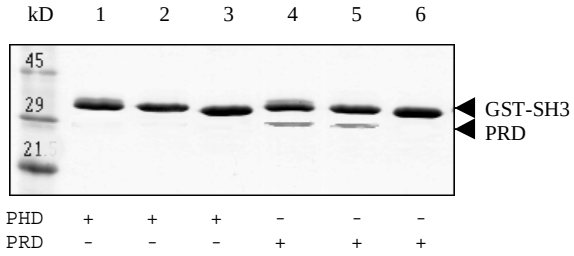

Figure 20. Binding of PRD but not PHD to GST-fusion proteins containing the SH3 domain of syndapin I (1 and 4), syndapin II (2 and 5) or on a SH3-mutant of syndapin I (3 and 6). Fusion proteins were immobilized on GST-agarose, then incubated with 5 µg PHD or PRD. After washing, bound proteins were eluted with SDS-containing buffer, analyzed by SDS-PAGE and stained with Coomassie blue.

3.5 Both PHD and PRD mediate binding of dynamin II to plasma membrane and Golgi membrane

Binding to the cytoplasmic phase of cellular membranes is an important feature of dynamins. Since the PHD of dynamin I binds to phosphoinositides(Zheng et al., 1996; Liu et al., 1994a), we first tested the ability of PHD to bind to total membrane lipids of bovine brain using a dot blot assay. As shown in Figure 21, strong binding was detected for PHD and PCP, whereas no detectable binding was observed using a control protein, the SH3 domain of amphiphysin II. This result was further confirmed by studing the binding of PHD to the plasma membrane and the Golgi membrane. Human erythrocyte inside-out vesicles prepared from ghost membranes (Sulpice et al., 1994) were used as a source of plasma membrane. Incubation with PHD resulted in strong binding (Figure 22, lane 2). In analogy, PHD could be bound to Golgi-enriched membranes of HepG2 cells (Figure 23, lane 6), suggesting that the existence of common membrane lipids both in the plasma membrane and in the Golgi membrane may form the binding sites for PHD. Also, the binding of PHD to the Golgi membrane was not significantly stimulated by GTP, ATP or cytosol (Figure 23, lane 7 and 8), hinting that this binding might be a PHD-lipid interaction without other protein involved. This was supported by a lack of proteins which bind to immobilized PHD (see 3.8).

==========

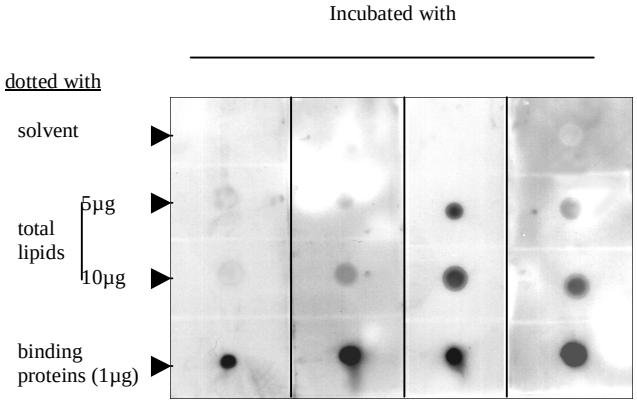

Figure 21. Binding of dynamin II domains to membrane lipids. 5-10 µg of total brain lipids in methanol/chloroform (1:1) were dotted onto NC membranes and incubated with GST-fused SH3 domain of amphiphysin II (SH3A), or PRD, PHD and PCP of dynamin II, respectively. Lipid bound proteins were detected with corresponding antibodies to GST (for SH3A), to *myc*-epitope (for PHD) or to dynamin II (for PRD and PCP). The assay was controlled by detection of the corresponding proteins (dots at bottom).

Since no data on membrane binding of PRD were known, we measured its binding to a total lipid mixture and membranes. Unexpectly, PRD bound to total brain lipids too (Figure 21), although the binding was less efficient than that of PHD. In the erythrocyte membrane binding assay, the binding was detectable but the extent was much lower in comparison to PHD (Figure 22, lane 1). As presumed, PRD alone or in presence of GTP/ATP bound to the Golgi membrane specifically but with relatively low efficiency (Figure 23, lanes 2 and 3). Nevertheless, the binding could be remarkably increased by addition of GTP/ATP and cytosol (Figure 23, lane 4) suggesting that some cytosolic components assisted this binding.

A comparison of the data shows that both domains may contribute to membrane binding of dynamin II: the PHD by interacting with lipids and the PRD by interacting with membrane proteins and/or with membrane lipids. The PRD binding proteins may contain SH3 domains, like syndapin, endophilin or a poly-proline binding proteins like profilin (Witke et al., 1998; Dong et al., 2000a). Binding of PRD to Golgi membranes specifically inhibited the constitutive formation of exocytic vesicles at the TGN (see 3.6.2).

==========

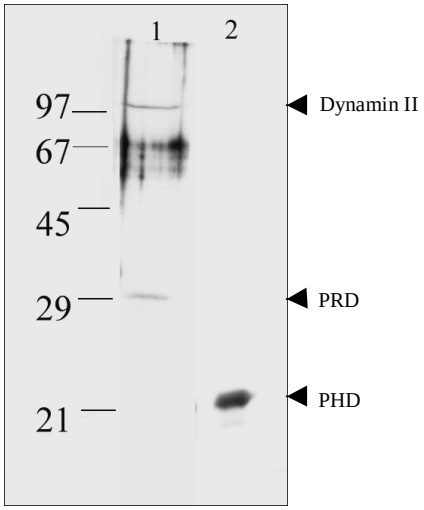

Figure 22. Binding of PHD and PRD of dynamin II to erythrocyte inside-out vesicles. Erythrocyte inside-out vesicles were incubated with purified dynamin II domains PRD (lane 1) or PHD (lane 2) and detected by anti-dynamin II (lane 1) or anti-*myc* (lane 2) antibody. In addition to PRD, endogenous membrane dynamin II (100 kD) was recognized.

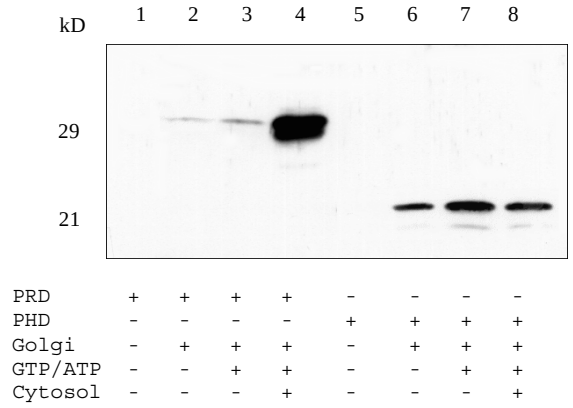

Figure 23. Binding of PRD (lanes 2-4) and PHD (lanes 6-8) to Golgi membrane of HepG2 cells. Golgi-enriched membranes (30 µg protein/assay) were incubated with 3 µg PRD or PHD and further supplements as indicated. Proteins bound to Golgi membrane were analyzed by SDS-PAGE and Western blotting. Minor band in lanes 7 and 8 indicate limited degradation during incubation. Assays 1 and 5 were controls.

==========

3.6 Impact of dynamin II and its domains on vesicle formation at the TGN

3.6.1 *In vitro* vesicle formation at the TGN

To study the role of dynamin II in vesicle formation at TGN, we used a modified *in vitro* assay to reconstitute the budding of vesicles with purified Golgi membranes (Westermann et al., 1996) on the basis of the method described by (Tooze and Stinchcombe, 1992). It has been known that heparan sulfate proteoglycans (HSPG) are sulfated in the TGN and transported via the constitutive secretory pathway to the plasma membrane (Stow et al., 1991; Rosa et al., 1992). While a portion of HSPG is finally distributed on the plasma membrane, another portion is directly secreted into the medium. The ratio of the two portions varies depending on cell type and culture condition. Since protein sulfation is a TGN specific posttranslational modification, measuring the amount of sulfated HSPG packed into vesicles allows us to assess the budding efficiency of constitutive vesicles at TGN. Therefore, HSPG represents a useful marker for studying the formation of post-Golgi vesicles. To perform this assay, HepG2 cells were labeled with [^{35}S]-sulfate *in vivo* and Golgi cisternae were purified, which contain sulfate-labeled HSPG. Upon incubation of Golgi cisternae with cytosolic proteins, GTP, ATP and an ATP-regenerating system at 37°C, the radiolabeled HSPG was packed into vesicles that can be separated from the starting Golgi membranes and quantified.

To reduce the budding background caused by randomly formed vesicles at the Golgi apparatus, purified intact Golgi membranes are required. We adopted a two-step gradient centrifugation to isolate Golgi membranes according to Beckers and Rothman (1992). The Golgi membranes were 80-100 fold enriched from the PNS as determined by analysing the TGN marker--galactosyltransferase (Westermann et al., 1996). The *in vitro* budding assay, which was performed in analogy to Tooze (1991), depends on energy supply in the form of ATP and GTP and is stimulated by cytosolic proteins. Cytosol dependence is an indication for the formation of new vesicles by the *in vitro* budding assay. Thus we first tested the requirement of cytosol and optimized the conditions. As shown in Figure 24, in the presence of full energy (see 2.2.14.2) and by incubation at 37 °C, the efficiency of vesicle budding from the Golgi-enriched membranes was significantly increased from 22 % to 42 % by addition of cytosolic proteins in the range of 40-200 µg/ml. Addition of more cytosol (up to 400 µg/ml) did not further elevate the budding level and may decrease vesicle budding at concentration of more than 1 mg/ml. In most cases, we used 100 µg/ml of

cytosol prepared from HepG2 cells. The background budding level which was measured by incubation of the same reaction system in ice was controlled to be less than 10 %.

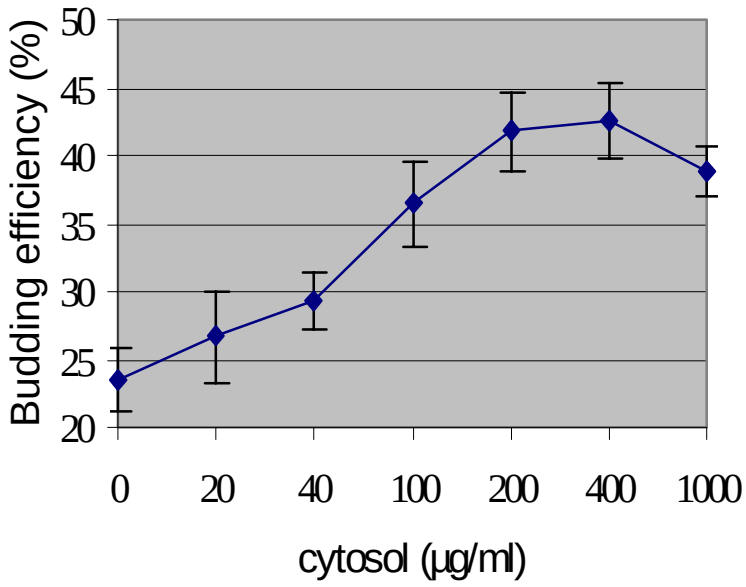

Figure 24. Formation of post-Golgi vesicles was stimulated by cytosolic proteins. The Golgi-enriched membranes were prepared from ^{35}S-sulfate-pulse labeled HepG2 cells and incubated with ATP, GTP and an ATP regenerating mixture at 37°C. Cytosolic proteins were added as indicated. HSPG containing vesicles were isolated and quantitated as described in 2.2.14.2.

3.6.2 Binding of PRD to the Golgi membranes inhibits formation of the constitutive vesicles at the TGN

To check the requirement of dynamin II for the formation of post-Golgi vesicles, we first observed the effect of a polyclonal antibody recognizing the C-terminus of dynamin II in the budding assay. As shown in Figure 25, the antibody effectively inhibited the formation of HSPG-containing vesicles which budded from the Golgi-enriched membranes. The budding level was reduced by about 70 % by anti-dynamin II antibody at concentration of 25 µg/ml. In contrast, the control antibody anti-VAMP2 at the same concentration did not affect vesicle budding. This suggests that dynamin II, the function of which has been blocked by its antibody, is required during the formation of post-Golgi vesicles. In a similar way, anti-pacsin II antiserum also inhibited vesicle formation, which may correlate

==========

to dynamin II (Figure 25). Since pacsin II (syndapin II) has recently been found to specifically interact with dynamin (Qualmann et al., 1999)(compare to 3.4) and is implicated in dynamin-mediated endocytic process (Qualmann and Kelly, 2000; Ritter et al., 1999), we supposed that dynamin II may form a complex with pacsin II or other proteins at the Golgi membrane sites that is required for vesicle formation.

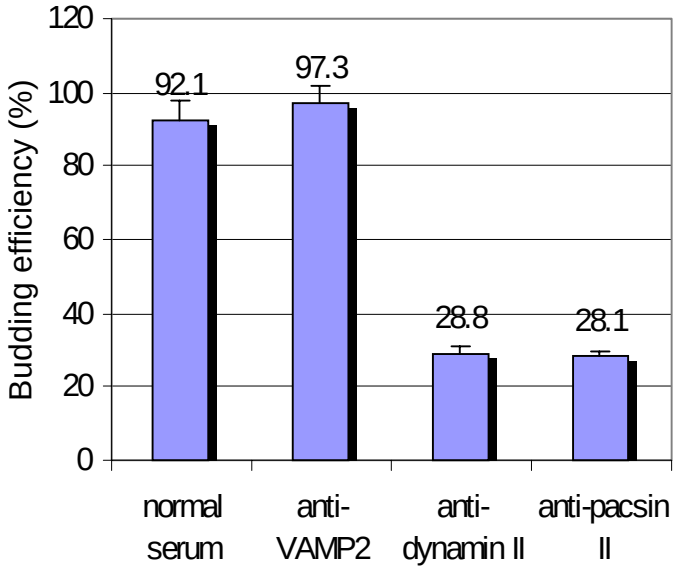

Figure 25. Inhibition of *in vitro* formation of HSPG-containing vesicles from Golgi-enriched membranes by the antibody to dynamin II or to pacsin II. Budding assays were performed in presence of 25 µg/ml (for anti-dynamin II IgG and anti-VAMP 2 IgG) or 1mg/ml (for anti-pacsin II antiserum or normal rabbit serum) of antibodies. Budding efficiency was measured according to 2.2.14.3.

PRD represents the domain of dynamin II which could mediate the interaction with SH3-containing proteins. Specific targeting of dynamin to the functional sites may largely depend on the interactions between PRD and its partners. To test the hypothesis that binding of dynamin II via its PRD is needed for vesicle formation, the purified PRD was added to the *in vitro* budding system and the formation of HSPG-containing vesicles was measured. Addition of increasing amount of PRD resulted in a remarkable reduction of the budding efficiency (diamonds in Figure 26). At a concentration of 100 µg/ml, the vesicle budding was reduced to about 45 % of the control level. In contrast, addition of the PHD of dynamin II at the same concentrations had no impact (squares in Figure 26). To identify if

==========

the inhibition was specifically caused by the PRD, the budding assays were preincubated with the purifed SH3 domain of amphiphysin II (SH3A) which has been shown to bind the PRD of dynamin II (see 3.4)(Grabs et al., 1997; Volchuk et al., 1998), before incubation with the Golgi-enriched membranes. The budding efficiency of formed vesicles was rescued to the original levels (triangles in Figure 26), suggesting that interactions between PRD and other proteins, which are required for inhibiting vesicle formation, were blocked by the interaction between PRD and SH3A. Interestingly, we did not observe any inhibition of vesicle formation by the SH3A alone (data not shown), indicating that functions of membrane bound dynamin II are insensitive to added SH3A. The reason could be an independence of the budding on amphiphysin II which has been found to be required for synaptic vesicle formation at nerve terminals but does not express in non-neuronal tissues (Ramjaun et al., 1997).

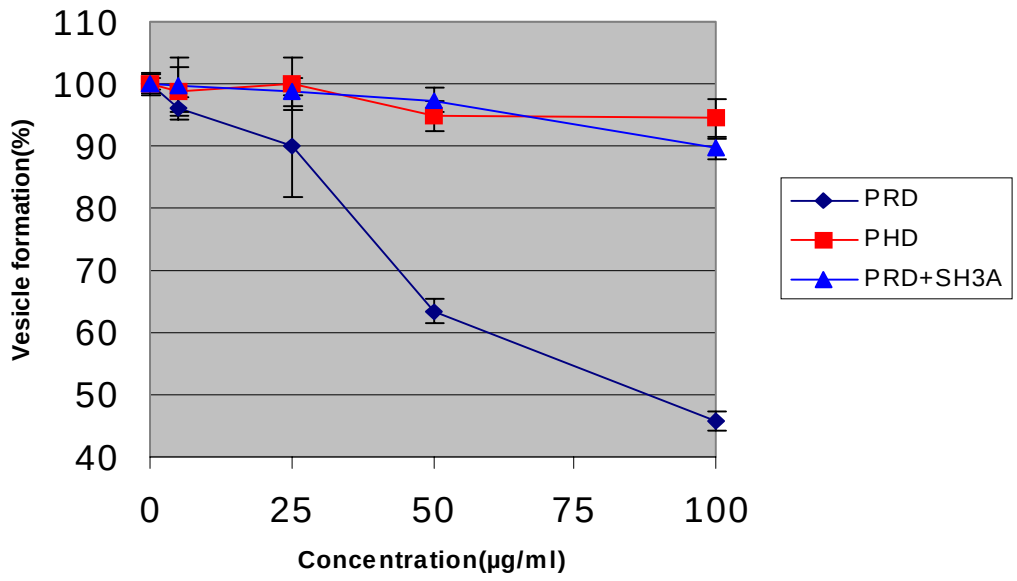

Figure 26. *In vitro* formation of HSPG containing vesicles at Golgi-enriched membranes was inhibited by PRD but not PHD of dynamin II. About 3-50 % of formed vesicles were inhibited by addition of 5-100 µg /ml recombinant PRD (diamonds). This inhibition could be reversed by addition of 50 µg/ml SH3 domain of amphiphysin II (SH3A, triangles). Addition of recombinant PHD (5-100 µg/ml, squares) had no effect.

==========

PRD of dynamin I has been found to stimulate the GTPase activity by interaction with microtubules and SH3-containing proteins such as Grb2, PLC-γ, and so on (Herskovits et al., 1993b). In addition, we have demonstrated that the recombinant PRD of dynamin II not only bound to SH3 domains but also interacted with membrane lipids (refer section 3.5). Interaction of PRD with membrane lipids may promote the binding of dynamin II to the membrane or directly stimulate the GTPase activity. Therefore, we suggest that the recombinant PRD might have competed with dynamin II to bind SH3-containing proteins and therefore reduced the GTPase activity of dynamin II which played a key role in releasing the vesicles. Also, because binding of the recombinant PRD to the Golgi membranes was strongly stimulated by cytosol (see 3.5), the binding sites on the Golgi membranes for endogenous dynamin II might be occupied by the added PRD, resulting in a decrease of membrane bound dynamin II (see 3.6.3).

3.6.3 Golgi-bound dynamin II was released by PRD

The inhibitory role of PRD on vesicle formation may result from competition with dynamin II for binding sites. We therefore studied the impact of PRD on the attachment of dynamin II on the Golgi membranes. Golgi-enriched membranes were prepared from HepG2 cells and incubated with purified PRD in low salt buffer (25 mM KAc) or in normal salt buffer (150 mM KAc). Thereafter, Golgi membranes were pelleted and the Golgi bound proteins were solublized in 2 % SDS-buffer, separated by SDS-PAGE and detected with anti-dynamin II antibody in Western blot asssay. Figure 27 showed that membrane-bound dynamin II was considerably detached from the Golgi membranes by incubation with recombinant PRD (lane 3 & 4), indicating that PRD interfered with the binding of dynamin II to the membrane sites. The candidate protein mediating binding of PRD to Golgi membrane could be an amphiphysin-like or an endophilin-like protein found in brain, but may also be profilin I because a detachment of dynamin II was also observed when a monoclonal antibody to profilin I was incubated with the Golgi membranes (lane 5 & 6) (Dong et al., 2000a). Profilin is a cytoskeleton protein that forms a complex with G-actin and regulates microfilament dynamics. Recent reports have demonstrated that profilin II is able to interact with proline-rich domain of brain dynamin I *in vitro* (Witke et al., 1998). Although we did not detected the significant binding of profilin I to dynamin II *in vitro*, profilin I was identified to be a Golgi bound protein and showed a colocalization with dynamin II *in vivo* (Dong et al., 2000a), suggesting that there may be a functional link

==========

between two proteins. The other protein which mediated the binding of dynamin II to the Golgi membranes may be syndapin II (pacsin II), which is located at Golgi and vesicular structures (Qualmann et al., 1999). The demonstration that antiserum of syndapin II inhibited the vesicle budding from the Golgi membranes *in vitro* (Figure 25) indicates an involvement of syndapin II. The interaction between syndapin II and dynamin II through SH3-PRD interaction, as shown in (Figure 20), may enhance the function of either or both of the proteins. We supposed that the recruitment of dynamin II to the Golgi membrane could be mediated by syndapin II or by profilin I, and the reduced efficiency of vesicle formation from the Golgi by the recombinant PRD was caused by replacement of membrane-bound dynamin II. In conclusion, the data again provided evidence that (1) dynamin II supports the formation of post-Golgi vesicles and (2) the PRD is essentail for the interaction between dynamin II and Golgi membrane.

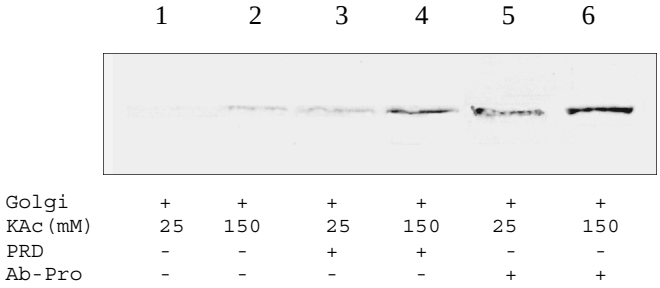

Figure 27. Dynamin II was released from Golgi membranes upon incubation with PRD. The Golgi-enriched membranes were incubated in buffer corresponding to the *in vitro* budding assay without further additions (lanes 1 and 2), with the PRD of dynamin II added (lane 3 and 4) or with a monoclonal antibody to profilin I (Ab-Pro) (lane 5 and 6) at 25 mM (lane 1, 3 and 5) or at 150 mM potassium acetate (lane 2, 4 and 6). Released proteins were separated by SDS-PAGE, blotted onto the NC membranes and probed with the antibody to dynamin II.

3.7 The impact of dynamin II domains on HSPG secretion by cultivated cells

3.7.1 PRD or PCP strongly inhibit secretion of HSPG by 293 cells

A function of PRD of dynamin II has been demonstrated by its inhibition of post-Golgi vesicle formation *in vitro*. To learn if a reduced packaging of HSPG into constitutive vesicles at the TGN may influence HSPG secretion, we established stable transfected 293

==========

cell lines that express dynamin II domains. To monitor the expression and study the intracellular localization, dynamin II domains were tagged with EGFP and then expressed under control of a tetracycline regulatable promoter. As the expression is inducible, possible toxicity to the cells due to long term overexpression of dynamin II domains could be prevented. While more than 99 % of cells were kept repressed, overexpression of dynamin II domains could be induced by addition of 1 µg/ml of tetracycline for 16-18 h. Induced cells were then pulse-labeled with [^{35}S]-sulfate in suspension because of poor attachment of 293 cells to culture dish. After labeling, free [^{35}S]-sulfate was washed away with cold DMEM to minimize the contamination of HSPG fractions with labeled [^{35}S]-sulfate. For kinetic study of secretion, cell suspensions were divided into equal aliquots and incubated in DMEM chase medium between 0 and 60 min at 37°C. The secreted HSPG and the intracellular HSPG were collected, precipitated with chondroitin sulfate and cetylpyridinium chloride, and quantitated by counting of radioactivity. First, we examined the amount of secreted HSPG and we studied the secretion dynamics in control 293 cells which express EGFP alone. As shown in Figure 28, the secretion of HSPG started immediately after shifting the cells to 37 °C and reached about 42 % within 15 min. Further secretion was slow and, at 60 min, reached about 50 % of the total HSPG. Because

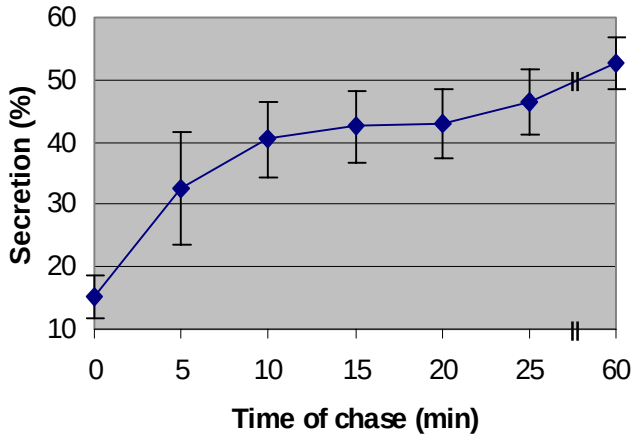

Figure 28. Kinetics of HSPG secretion. Secretion of HSPG by 293 cells expressing EGFP, which was used as a control for secretion assays, was analyzed as described in 2.2.15. The data (mean ± SD) are the average of four independent experiments.

==========

a portion of HSPG remained attached to the plasma membrane and was therefore found in the cell pellet (Stow et al., 1989) (Soroka and Farquhar, 1991), the secretion of soluble HSPG may be complete after 60 min of incubation and could represent the total level of secretable HSPG.

In comparison to control 293 cells which express EGFP, the secretion of HSPG from 293 cells expressing PRD or PCP was notably supressed (Figure 29). The secretion was slowed down remarkably at early stage (10 min) where, compared with control cells, secretion of HSPG was suppressed by 27.2%, 38.9% and 58.2% by PHD, PRD and PCP, respectively (Table 4). At late stage (25 min), the corresponding suppressions were attenuated to 16.8%, 25.0% and 28.4%, respectively, but the secretion levels were still lower than that of control cells. Contrary to *in vitro* budding assay where the recombinant PHD did not affect vesicle formation at the TGN (see section 3.6.2), the expression of PHD resulted in a moderate suppression of HSPG secretion (Figure 29). This finding suggests that overexpression of PHD also impair secretion function of cells. Two effects may be responsible for the discrepancy: first, the *in vitro* kinetics of vesicle formation could also be reduced but was not determined; second, inhibition of other steps than vesicle formation

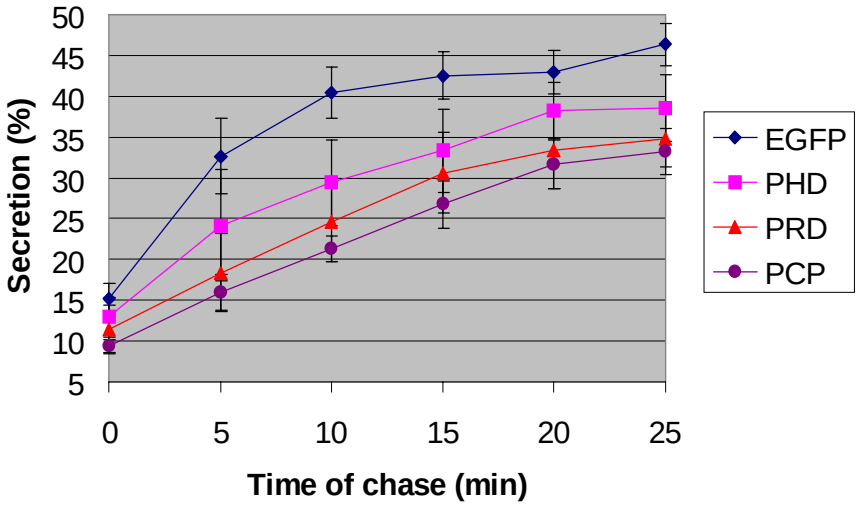

Figure 29. Impacts of dynamin II domains on the secretion of HSPG. Kinetics of HSPG secretion from 293 cells expressing EGFP (diamonds) or EGFP-tagged dynamin II domain PHD (squares), PRD (triangles) and PCP (dots) were measured as described in 2.2.15. The data (mean ± SD) are the average of four independent experiments.

==========

may result in a reduced *in vivo* secretion. Since HSPG secretion is a stepwise process including sulfation, sorting, transport and fusion of vesicles to the plasma mebrane, disruption of any single step will affect but may hardly block the secretion. Overexpression of PHD may prevent the fusion of secretory vesicles with plasma membrane by interaction with membrane lipids (Figure 21), such as $PI(4,5)P_2$, whereas PRD of dynamin II may reduce the secretion speed of HSPG by specific inhibition of vesicle formation at the TGN. The most potent suppression of HSPG by PCP represented the combined effects from PHD, GED and PRD that may have impacts on different steps of vesicle formation.

Table 4. Comparison of impacts of dynamin II domains on secretion of HSPG by 293 cells at 10 min and 25 min incubation.

	10 min		25 min	
Domain	secretion (%)	inhibition (%)	secretion (%)	inhibition (%)
Control(EGFP)	40.4	0	46.4	0
PHD	29.4	27.2	38.6	16.8
PRD	24.7	38.9	34.8	25.0
PCP	21.3	58.2	33.2	28.4

3.7.2 Reduced secretion of HSPG correlates with reduced dynamin II attached to the Golgi

Because vesicle formation at TGN is an important process during protein secretion, disruption of the machinery containing dynamin II at the Golgi membranes could affect the secretion speed. To study whether the reduced secretion of HSPG from dynamin II domain-expressing cells was caused by replacement of Golgi bound dynamin II, we analyzed the distribution of EGFP-tagged dynamin II domains and membrane-bound endogenous dynamin II at Golgi membranes. For this purpose, the Golgi-enriched membranes were prepared from stable transfected 293 cell as described in 2.2.13. Thereafter, the membrane bound proteins were solubilized in 2% SDS-containing buffer and analyzed by Western bloting. Golgi-enriched membranes were quantitated by a Golgi specific protein -- syntaxin 6 (Figure 30). The result showed that all three dynamin II domains were able to bind Golgi membranes. In contrast, the EGFP alone did not or weakly bound to the Golgi. Interestingly, although the binding of PHD to the Golgi membranes was stronger than PRD and PCP, the amount of membrane-bound dynamin II was unaffected. Therefore, the effective binding of PHD to the Golgi and to the plasma membrane may not reduce budding efficiency at Golgi but may cause a blockage of vesicle

==========

fusion with plasma membrane. On the contrary to PHD, binding of PRD or PCP to the Golgi membranes significantly reduced the amount of membrane-bound dynamin II (Figure 30), which may correlate with their ability to suppress HSPG secretion (compare to Figure 29). The data suggest that the C-terminal domain of dynamin II plays an important role in vesicle formation.

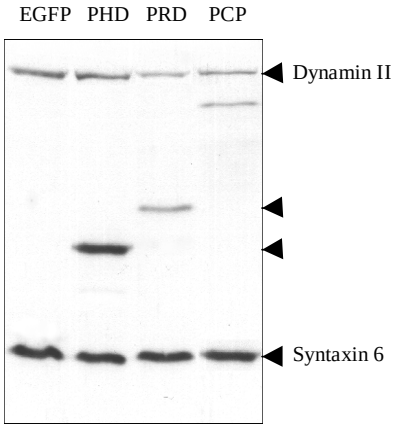

Figure 30. Binding of dynamin II domains to Golgi membrane and detachment of endogenous dynamin II from Golgi by PRD and PCP. Golgi-enriched membranes prepared from 293 cells overexpressing EGFP alone or EGFP-tagged dynamin II domain EGFP-PHD, EGFP-PRD and EGFP-PCP were analyzed by SDS-PAGE and Western blotting. EGFP-tagged proteins were detected with an anti-*myc* antibody, the endogenous dynamin II with an anti-dynamin II antibody, and the Golgi marker protein, syntaxin 6, with an anti-syntaxin 6 antibody.

3.8 Dynamin II binding proteins

In the last decade, most infomation about proteins interacting with dynamin family have been obtained from neuron specific dynamin I, whereas the proteins which bind to dynamin II, the ubiquitously expressed form of dynamin, are unknown. To study the mode of action of dynamin II at the Golgi, the PRD, which is believed to mediate protein-protein interactions and shares the lowest homology between dynamin isoforms, was used to study the binding proteins. Using protein affinity binding assay, we identified binding proteins which differ between dynamin I and dynamin II as well as those common to both isoforms.

==========

3.8.1 Proteins of rat brain that bind to PRD

Since the inhibitory effect of PRD on vesicle formation at the TGN may depend on binding of cytosolic or membrane proteins, we identified proteins which bind to this domain. For this purpose, purified his-s-PRD was attached to S-protein agarose. The formed S-peptide - S-protein complex immobilizes the PRD to the matrix and makes it possible to analyze protein binding under stringent conditions. To optimize the method and to compare the result with recent data on binding of proteins from rat brain to the PRD of dynamin I (Slepnev et al., 1998), we started the study by binding of proteins extracted from rat brain homogenates with 1 % Triton X-100. After incubation of matrix-attached PRD with protein extracts in 50 mM NaCl, 20 mM HEPES-KOH, pH 7.5, and 1 % Triton X-100, and removing unspecifically bound proteins with the same buffer containing 300 mM NaCl, the bound proteins were eluted together with the PRD by an SDS-containing buffer. Separation by SDS-PAGE resulted in a distinct pattern of binding proteins. After blotting the proteins onto NC membrane, the identity of the main bands was determined by immunoblotting. The most prominent bands represented amphiphysin I and syndapin I that have been studied *in vitro* by their SH3 domains. In addition, signals of clathrin, α-, β- and γ-adaptin, EEA1 as well as p47A and β-tubulin were detected (Figure 31 and Table 5). No binding of EPS15 and AP180, which were shown to indirectly interact with the PRD of dynamin I (Slepnev et al., 1998), were observed. The binding to α- or β-adaptin could be either direct via the hinge region (Wang et al., 1995) or indirect by binding to amphiphysin (Slepnev et al., 1998). γ-adaptin is a subunit of AP-1 which associates with the TGN and links selected membrane proteins to the clathrin lattice (Lewin et al., 1998; Robinson, 1990). Our data indicate that γ-adaptin, like α-adaptin of AP-2 binding to dynamin I, may participate in recruitment of cytosolic dynamin II to the TGN either directly or through protein complex since a direct interaction between γ-adaptin and dynamin II has never been reported before. Also, no evidence was published for interaction between dynamin II and p47A which lacks an SH3 domain. p47A is a subunit of the AP-3 complex (Pevsner et al., 1994b) which is involved in protein sorting to lyosomes (Faundez et al., 1998; Salem et al., 1998). Detection of p47A (Figure 31) suggests an indirect attachment to the PRD via unknown binding proteins.

Syndapin I is a brain specific protein that is involved in multiple protein-protein interactions. It interacts with the brain-specific dynamin I, synaptojanin, and synapsin I via

==========

its SH3 domain (Qualmann et al., 1999). Association of syndapin I with dynamin I *in vivo* may play a role in synaptic vesicle endocytosis (Qualmann and Kelly, 2000). Here, the binding of syndapin I to the PRD of dynamin II suggests that some membrane proteins are common to endocytic and exocytic machineries.

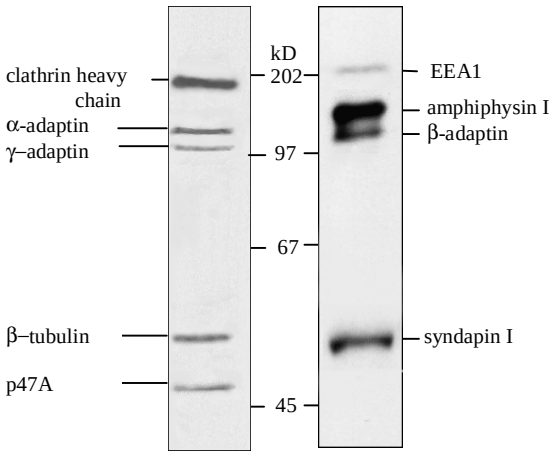

Figure 31. Proteins of rat brain extract that bind to PRD. Purified PRD of dynamin II was immobilized on S-protein agarose, then incubated with rat brain extract at 4° for 2 h. After extensive washing, bound proteins were eluted with 2% SDS sample buffer and separated by SDS-PAGE and analyzed using specific antibodies in Western blotting.

To identify more proteins bound to PRD, proteins were separated by SDS-PAGE and the gel was stained with silver. Protein bands distinct from the identified proteins mentioned above were selected. In this way, six proteins have been identified (Table 5). One of them, SH3GL2 (also called endophilin I), is a SH3 domain containing protein which is exclusively expressed in brain (Giachino et al., 1997). It has been found to interact with amphiphysin I (Micheva et al., 1997a) and synaptojanin I (Cestra et al., 1999) as well as with dynamin I (Schmidt et al., 1999), and may serve as an important member of a biochemical machinery that acts in synaptic veiscle formation (Ringstad et al., 1999; Micheva et al., 1997b). As proteins involved in endocytosis may also be used in exocytosis in brain, the binding of SH3GL2 to the PRD of dynamin II suggests that the dynamin II functions in both pathways in brain.

Another identified protein is STX-1 - a syntaxin binding protein that interacts with syntaxin (Hata and Sudhof, 1995) and SNAP-25 (Chapman et al., 1994). It determines the

==========

specificity of intracellular fusion reactions both in synaptic endocytosis (Hata et al., 1993; Hata et al., 1993) and exocytosis (Shuang et al., 1998; Jacobsson and Meister, 1996). STX-1 contains a GTP binding domain but lacks a SH3 domain, which suggests an indirect binding to the PRD via unknown proteins.

In addition, the NEM-sensitive factor (NSF) was identified by microsequencing of bound proteins. NSF is a member of the ATPase superfamily and has been reported to be required for membrane fusion (Nichols and Pelham, 1998; Burgoyne and Morgan, 1998). Since there has not been any evidence for direct interaction between NSF and dynamin, it probably associated with PRD via other proteins.

GRP75 is a stress-inducible mitochondrial chaperon which implicated in the control of cell proliferation and cellular aging (Merrick et al., 1994; Webster et al., 1994). Recent study shows that GRP75 could form a complex with mutant p53 in cytoplasma and may affect the subcellular distribution of p53 protein (Merrick et al., 1996). Also, dynamin II has been recently found to induce apoptosis in a p53 dependent manner (Fish et al., 2000). Whether GRP75 links dynamin II to p53 by forming a protein complex to regulate the apoptosis is hypothetical.

From the experiment above, we detected common as well as different binding proteins of dynamin I and dynamin II (Table 5). Interaction with SH3 containing proteins (amphiphysin I/II, syndapin I/II, endophilin I etc.) represents the direct binding to the PRD. But binding of proteins that lack a SH3 domain (γ-adaptin, p47A etc.) indicates that protein complexes contains at least one protein with a SH3 domain.

3.8.2 Proteins of HepG2 cells that bind to PRD

In Western blot experiments, clathrin heavy chain, α-adaptin, β-adaptin, γ-adaptin, EEA1 and p47A from HepG2 cell extracts were detected to bind to PRD (Table 5). The signal for β-adaptin has to be further specified since the antibody may recognize β1- or β2-adaptin which may either indicate binding of AP1 or AP2 complex. Instead of syndapin I, which is exclusively expressed in brain, the homologous syndapin II [also called pacsin II (Ritter et al., 1999)], which is expressed in peripheral tissues, has been detected. Syndapin II binds to the Golgi apparatus and colocalizes with dynamin II (Qualmann and Kelly, 2000). Recent reports show that the SH3 domain of syndapin I or syndapin II was able to inhibit receptor-mediated internalization of transferrin, suggesting an involvement in endocytosis *in vivo* (Qualmann and Kelly, 2000). Although at present the functions of syndapin II is not

==========

clear, inhibition of vesicle formation by antibodies that recongnize this protein allows us to predict that a machinary composed of syndapin II, dynamin II and other proteins may have an impact on vesicular traffic in non-neuronal cells.

Since a relatively large number of proteins from rat brain extract bind to PRD of dynamin II, the effect of individual protein on vesicle formation could not be tested. To reduce diversity of binding proteins, we used proteins extracted from Golgi-enriched membranes. Under conditions optimized for binding of rat brain proteins, the Golgi membrane proteins that bind PRD-agarose were analyzed. Four prominent bands were mass-spectometrically sequenced:

- A protein band of 86 kD was identified as S23A, a component of the COPII coat protein complex, which may attach to the cis-Golgi (Paccaud et al., 1996). COPII is composed of at least five proteins: the SEC23/24 complex, the SEC13/31 complex and the protein SAR1. Unlike COP I coat, COP II coat acts in the cytoplasm to promote the transport of secretory proteins, plasma membrane proteins and vesicular proteins from the endoplasmic reticulum to the Golgi complex (Kuehn et al., 1998; Springer and Schekman, 1998). There is neither evidence that dynamin II is involved in formation of COP II vesicles nor evidence that dynamin II interacts with S23A. Thus, the nature of this bound complex is unknown.
- A 75 kD band contains sequences of dynamin II and may represent a truncated form of the 100 kD protein. Origin and function of this protein are unknown.
- A 57 kD band was identified as protein disulfide isomerase, a chaperon-like protein, which binds to (partly) denaturated proteins and may not represent a specific ligand of the PRD.
- A protein band of about 240 kD containing Pyr1_human, a trifunctional enzyme of the pyrimidine synthesis pathway with no obvious relation to vesicle biogenesis.

Comparing PRD binding proteins of brain and HepG2 cell extracts shows a general similarity (Table 5). Some protein isoforms differentially express in tissues and therefore were identified from different tissues. For example, amphiphysin I, syndapin I and endophilin I are expressed specifically in brain, while syndapin II and adaptins are ubiquitously expressed. Additionally, some proteins identified by microsequencing method do not contain SH3 domain, suggesting that these proteins may form complexes with PRD or interact with PRD via a unknown domain. Identification of binding specificity and functions of these proteins in vesicle traffic are of interet.

==========

Analysis of binding proteins of dynamin II suggested that vesicle formation is a complex process involving many proteins and membrane lipids. Dynamin II functions mostly at late stage of vesicle budding and it is required to form a protein complex (s) for release of the formed vesicles. Since dynamin I is only expressed in neuronal cells and is an essential protein for the formation of synaptic vesicles, the ubiquitouly expressed dynamin II may play roles in both endocytosis and exocytosis in non-neuronal cells. The interaction of PRD with three types of adapor complexes supported this notion. Moreover, interaction between EEA1 and PRD of dynamin II prompts that the recycling of endocytosed membrane proteins like receptors or membrane lipids from the early endosomes to the plasma membrane may depend on dynamin II. Finally, the binding of β-tubulin to PRD also proved the direct interaction between dynamin II and microtubules. Function of other binding proteins for PRD, especially syndapin II/pacsin II is under investigation.

Table 5. Proteins bound to the PRD of dynamin II [1)]

Proteins bound (Protein source: rat brain)	Identified by	Proteins bound (Protein source: HepG2 cells)	Identified by
Clathrin	Western blotting	Clathrin	Western blotting
Amphiphysin I	Western blotting	n.d.[2)]	
α-adaptin	Western blotting	α-adaptin	Western blotting
β-adaptin	Western blotting	β-adaptin	Western blotting
γ-adaptin	Western blotting	γ-adaptin	Western blotting
Syndapin I	Western blotting	Syndapin II	Western blotting
SH3GL2(endophilin)	Protein microsequencing	n.d.	
Syntaxin-binding protein	Protein microsequencing	n.d.	
NEM-sensitive vesicular fusion protein (NSF)	Protein microsequencing	n.d.	
		S23A	Protein microsequencing
β-tubulin	Western blotting	n.d.	
EEA1	Western blotting	EEA1	Western blotting
P47A	Western blotting	P47A	Western blotting

[1)] Only those proteins were listed which may have an impact on vesicle biogenesis.

[2)] Amphiphysin I, abundantly expressed in rat brain, was not detected in rat liver Golgi.

==========

3.9 Intracellular localization of dynamin II and its domains

The subcellular localization of dynamin I and II has been characterized by using immunoelectron microscopy and confocal microscopy with EGFP fusion proteins (Cao et al., 1998b; Maier et al., 1996; Herskovits et al., 1993a). In addition to the cytoplasmic pool, most dynamin I is bound to plasma membrane where it associates with clathrin coated pits (Damke et al., 1994; Baba et al., 1999). Although the bb variant of dynamin I showed a partial localization to Golgi apparatus (Cao et al., 1998b), there is no evidence of a function of dynamin I at Golgi, so far. In case of dynamin II, the localization was more heterogenous. While the spliced variants aa and ba predominantly attached to the Golgi apparatus, the spliced form ab and bb, which differ respectively in only four amino acid residues to aa and ba forms, do not localize to Golgi (Cao et al., 1998b). Different localizations of dynamin III spliced forms have also been observed (Cao et al., 1998b). This implys that different primary structures may affect the localization of dynamin spliced variants. Dynamin II has two splicing regions that generate 4 variants (Figure 3). The PHD and PCP constructs in the present study covered the second splicing area, representing the bb variant. The C-terminal PRD, however, is common to all dynamin II spliced forms.

Firstly, the localization of endogenous dynamin II in HeLa and Cos cells was studied by using antibodies to dynamin II. In order to reduce the cytosolic staining caused by the cytosolic pool of dynamin II, cells were permeabilized before fixation. Notably, we found two types of localization for dynamin II in HeLa and Cos-7 cells. One type displayed a Golgi dominant staining which colocalized with Golgi marker—TGN38 (Figure 32 a-a´´), whereas the other type showed a more broad distribution including plasma membrane and Golgi membranes (Figure 32 b-b´´, Figure 34 a, b and c). This may represent the detection of different spliced variants of dynamin II which were recognized by different anti-dynamin II antibodies. The monoclonal antibody to dynamin II (Transduction Laboratory), used in Figure 32 a, may recognize specifically one of the spliced variants which may attached to the Golgi. The polyclonal antibody to dynamin II, used in Figure 32 b, recognizes the C-terminal peptide (see 2.1.1) which is common to all spliced variants of dynamin II (compare Figure 3). The latter therefore recognized all variants of dynamin II expressed in HeLa cells, giving rise to a broad staining.

==========

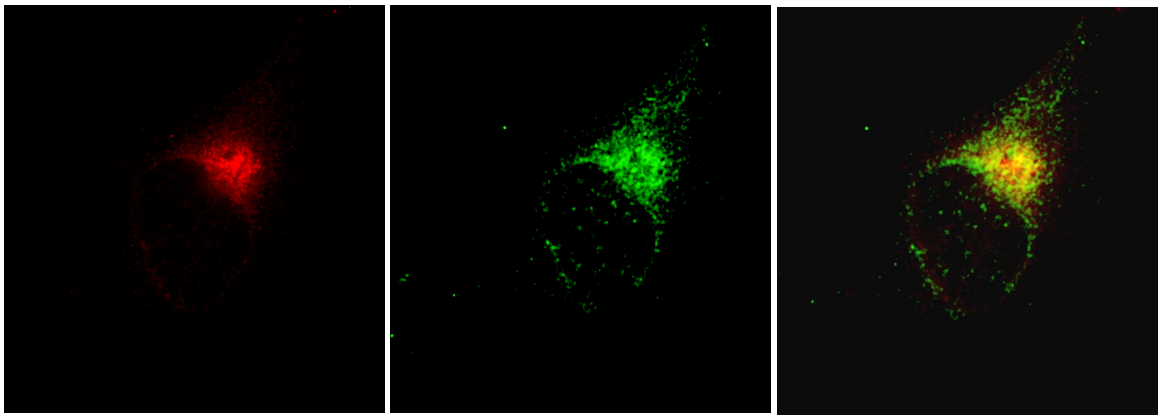

dynamin II TGN38 overlay

b b´ b´´

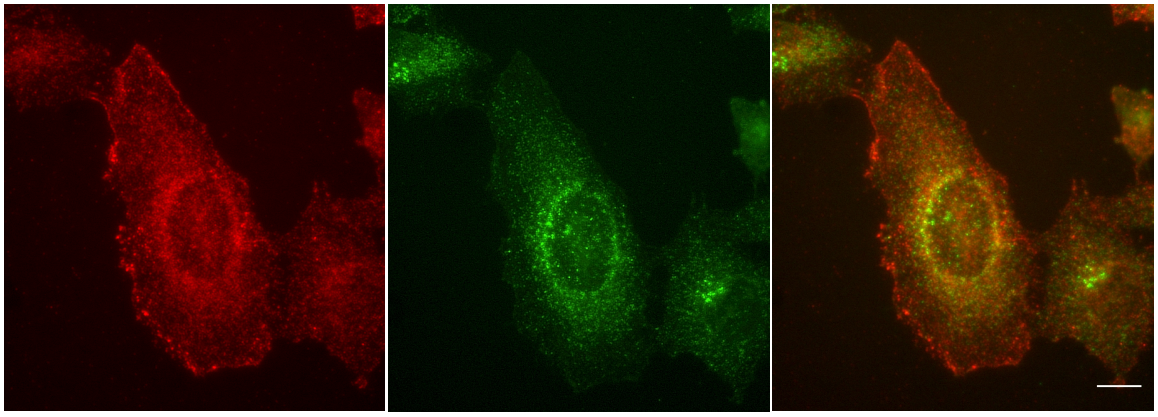

dynamin II γ-adaptin overlay

Figure 32. Distribution of endogenous dynamin II in HeLa cells. HeLa cells were permeablized before fixation and double immunostained with antibodies to dynamin II (a and b) and to Golgi marker TGN38 (a´) or γ-adaptin (b´) as described in Materials and Methods. The separate images were overlaid in a´´ or b´´, respectively, to view colocalization. Bar = 10 µm

==========

To elucidate the localization of individual domain of dynamin II, we constructed plasmids containing dynamin II domains tagged with C-terminal EGFP as a reporter protein. Using calcium phospate precipitation method, plasmids containing EGFP alone or EGFP-tagged PHD, PRD and PCP were transiently transfected into HeLa or COS-7 cells. The expression of all three domains could be observed at 8-10 h after transfection. The maximum expressions required 18-36 h incubation. After fixation with ice-cold methonal/acetone (1:1), the cells were imaged with fluorescence microscopy. The distinct localization of three domains was observed. Cells expressing EGFP alone displayed a diffuse fluorescence throughout the cytoplasm and nucleus (Figure 33, EGFP-C1). Whereas cells expressing EGFP-PHD protein revealed a prominent localization to the perinuclear area and plasma membrane (EGFP-PHD). Obviously, most of EGFP-PRD was observed at the Golgi apparatus (EGFP-PRD) and was similar to the distribution of endogenous dynamin II in HeLa cells (compare to Figure 32).

Interestingly, unlike PHD and PRD, expression of the C-terminal half of dynamin II (EGFP-PCP) attached to punctate or granular structures in cytoplasm or nucleus. The size of these structures varied from 0.1 to 5 μm in diameter and became more aggregated after induction for over 24 h. To investigate whether these structures were derived from cell organelles, the cells were immunostained with antibodies to marker protein of the TGN (TGN38, syntaxin 6 and γ-adaptin), of lysosomes (LAMP-1), of endoplasmic reticulumn (BiP/GRP78) and of endosomes (EEA1). Mitochondrions were identified by MitoTracker Red CMXRos (Molecular Probe). In no case was a colocalization with marker protein observed. Whether these structures were formed by self aggregation or represent other special subcellular structures correlated to cell functions is presently being studied.

The subcellular localization of three dynamin II domains in stable transfected 293 cells showed a similar result

Although the location of PRD was similar to that of endogenous dynamin II in HeLa cells, we did not find a complete overlap. Therefore, we suggest that the localization of dynamin II requires the coordination of all domains. Contribution from individual domains by interacting with membrane components (via PHD), memrane proteins (via PRD) or even the GTPase domain (Labrousse et al., 1998) may determine the final destination of dynamin II protein.

==========

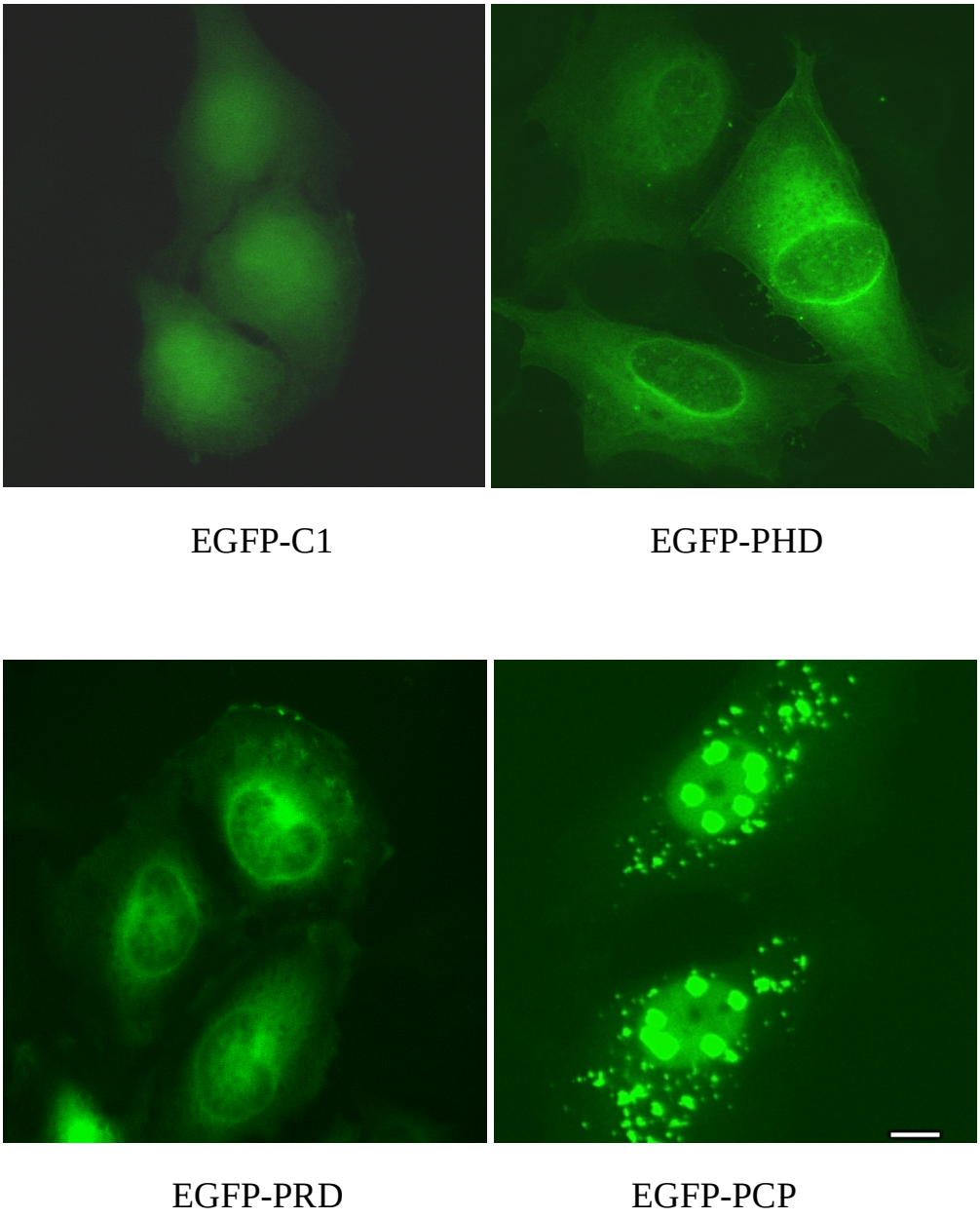

Figure 33. Localization of dynamin II domains in HeLa cells. EGFP alone or EGFP-tagged dynamin II domain EGFP-PHD, EGFP-PRD and EGFP-PCP were expressed in HeLa cells by use of pEGFP-C1 vector constructs. Cells were incubated for 24 h after transfection and fixed with methanol/acetone (1:1). Localization of EGFP-fusion domains was analyzed by confocal fluorescence microscopy. The vector pEGFP-C1 was used as a control. Bar = 10 µm

==========

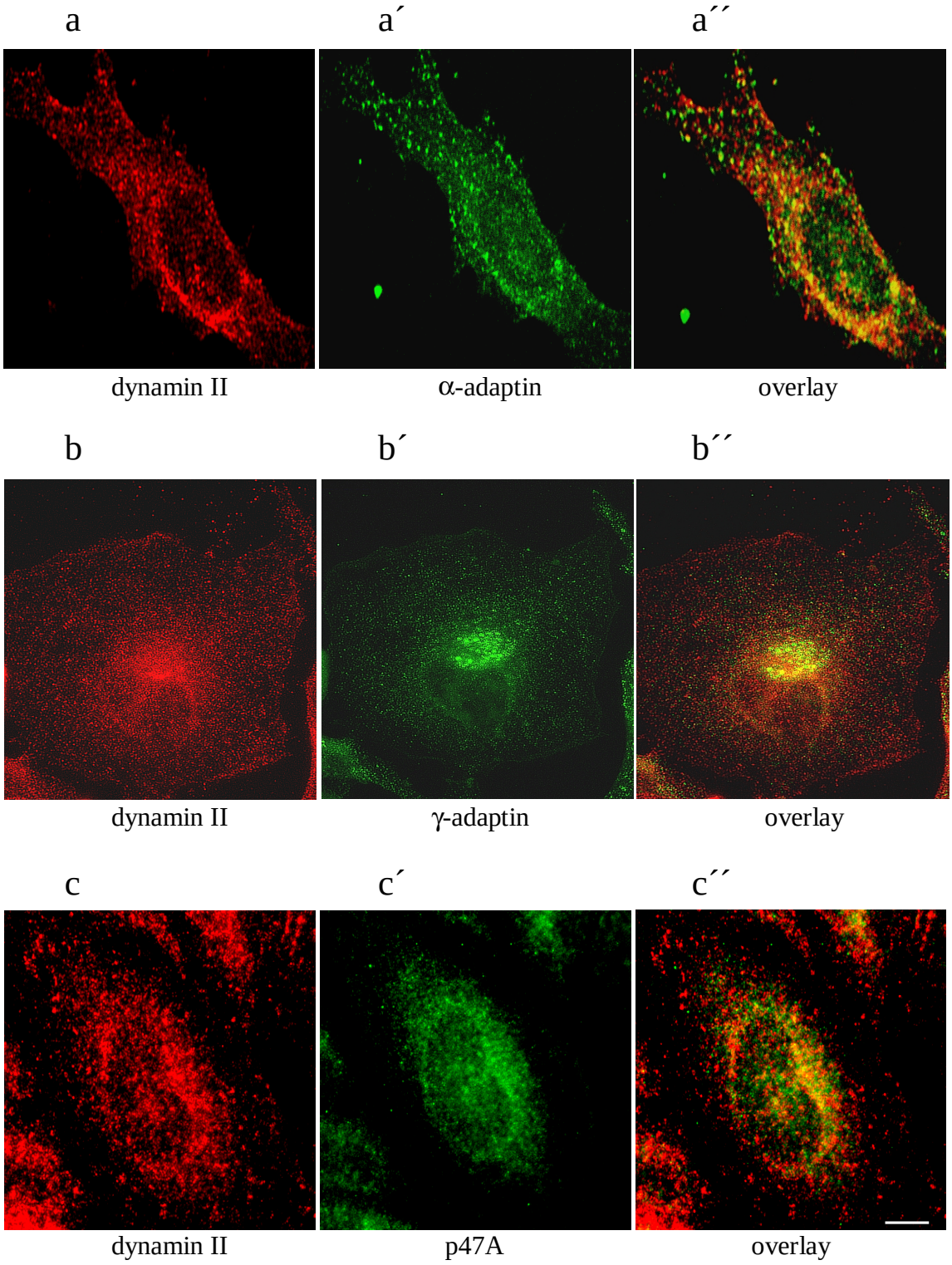

Figure. 34. Colocalization of dynamin II with adaptor proteins in HeLa cells. Transfected cells were immunostained with a polyclonal antibody to dynamin II (a, b and c) and the monoclonal antibody to α-adaptin (subunit of AP-1), to γ-adaptin (subunit of AP-2) or to p47A (subunit of AP-3) as indicated. Colocalizations were shown in overlays. Bar =10 µm.

==========

The adaptor proteins, such as α- and β-adaptin of AP-2, γ-adaptin of AP-1 and p47A of AP-3, bind *in vitro* to recombinant PRD (see 3.8) promoted us to study the colocalization of dynamin II with these adaptins by double immunostaining and confocal microscopy. Partial colocalizations of dynamin II with all three adaptins were observed (Figure 34). α-adaptin was bound to vesicular structures throughout the cytoplasm and showed limited colocalization with dynamin II (Figure 34, a-a´´). γ-adaptin and p47A were more concentrated in the Golgi area and showed more overlaps with dynamin II (Figure 34, b-b´´ and c-c´´). Importantly, the data may suggest that dynamin II participates in vesicle formation which is mediated by either of three adaptor complexes. It can also be assumed that different spliced variant of dynamin II interacts with different adaptor complex at different sites.

3.10 The assembly of dynamin II is inhibited by PRD and PCP

Members of dynamin family have the tendency to self-assemble under low salt conditions (Hinshaw and Schmid, 1995; Warnock et al., 1996; Wienke et al., 1999), which may represent a lipid membrane-deforming property. Dynamin I has been found in a tetrameric form in the cytosol (Muhlberg et al., 1997). Further polymerization of dynamin I tetramers results in the formation of spirals around liposomes *in vitro* (Sweitzer and Hinshaw, 1998; Takei et al., 1998) or at invaginated plasma membrane buds *in vivo* (Takel et al., 1995; Baba et al., 1999). Although the functional meaning of polymerization is unclear, it is

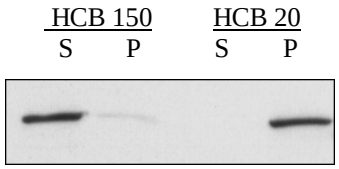

Figure 35. Cytosolic dynamin II becomes sedimentable upon dialysis against low salt buffer. Cytosol from 293 cells was dialyzed in low salt buffer (HCB 20) or physiologic salt buffer (HCB 150) for overnight, then centrifuged at 150,000 g for 15 min. Dynamin II in pellets (P) and supernatants (S) were detected by anti-dynamin II antibody.

==========

supposed that the formation of dynamin ring structures around vesicles may mediate vesicle scission (Hinshaw, 1999). But collar-like structures of dynamin are hardly observed *in vivo* because they may represent a short-lived form during vesicle formation. Recently, some laboratories have demonstrated that self asssembly of dynamin *in vitro* could be induced by dialyzing purified dynamin against low salt buffer (Warnock et al., 1996). We observed that the cytosolic dynamin II from 293 cell or HepG2 cell formed a sedimentable complex in low salt buffer HCB 20 (Figure 35). More than 90 % of cytosolic dynamin II was pelleted after centrifugation at 100,000 g for 15 min. In contrast, only a small portion (less than 5 %) of dynamin II was sedimented after dialysis against physiological salt buffer HCB 150. Though composition and structure of this sedimentable form is unknown, it suggests an ability of dynamin II to assemble into large complexes which eventually may have biological functions.

To explore the role of individual domain in dynamin II assembly, we analyzed the endogenous dynamin II in cytosolic fractions from 293 cells overexpressing EGFP-tagged dynamin II domains. Cytosolic fractions prepared from these cells were used for assays of dynamin II assembly. As shown in Figure 36, the low salt buffer-induced dynamin II assembly was strongly inhibited by the presence of PRD or PCP but was not affected by EGFP alone or PHD. The finding suggests that the PRD of dynamin II participates in assembly. This notion is supported by the observation that truncated dynamin I, which lacks the PRD, lost the ability to assemble (Muhlberg et al., 1997). Since interaction between PRD and other domain of dynamin II are not documented, it is speculated that SH3 domain proteins may be involved. PHD, however, is not required for assembly of dynamin II.

As evidence has demonstrated that polymerization of dynamin is a precondition to deform liposomes to tubules (Tuma and Collins, 1995) and is an effector of its intrinsic GTPase activity (Warnock et al., 1996), the data here support the hypothesis that the inhibition of dynamin II functions in vesicle formation at the TGN by PRD or PCP may result from the disturbance of self-assembly of dynamin II in addition to the detachment of membrane-bound dynamin II.

==========

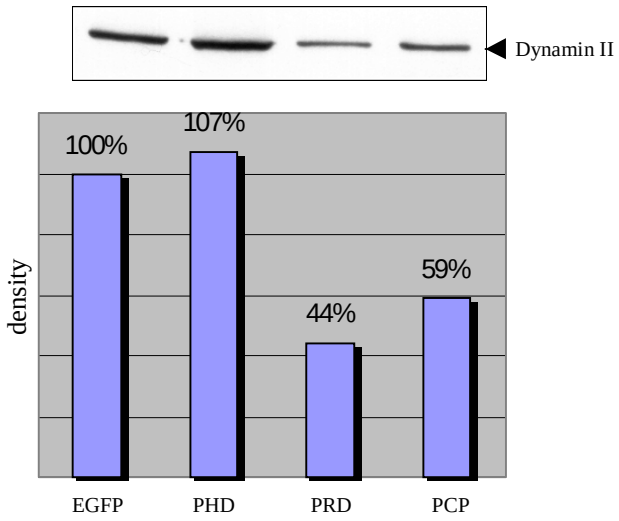

Figure 36. Inhibition of dynamin II assembly in the presence of PRD or PCP. Dynamin II assembly was tested using cytosol from 293 cells overexressing EGFP alone or EGFP-tagged dynamin II domain, EGFP-PHD, EGFP-PRD and EGFP-PCP, respectively. Sedimentable dynamin II was detected by SDS-PAGE and Western blotting using an anti-dynamin II antibody (upper panel). Density of bands was scanned and documented in the low chart.

==========

IV Major contributions to the structure and function of dynamin II

This study was focused on the structure of dynamin II domains and their impact on functions of dynamin II in vesicle formation at the TGN. In addition to known data some of which have been published during the study, four major contributions have been made :

1. Analysis of fluorescence and CD spectra of the recombinant PHD of dynamin II revealed a well-folded globular protein containing β+α mixed structures, which is similar to the PHD of dynamin I. This may suggest that binding to membrane lipids, as well as the lipid-dependent stimulation of GTPase activity, are conserved in dynamin I and dynamin II. In addition, the first evidence was obtained that the PRD represents an unfolded domain, which, nevertheless, preserved the ability to bind SH3 domain proteins.
2. Dynamin II is required for the constitutive formation of secretory vesicles at the TGN. In an *in vitro* budding assay, recombinant PRD of dynamin II, as well as a specific antibody to dynamin II, strongly inhibited the formation of HSPG-containing vesicles at the TGN. Accordingly, the secretion of HSPG by living cells was moderately suppressed by overexpression of the PHD of dynamin II. Overexpression of PRD or PCP strongly inhibited the secretion and simultaneously released dynamin II from the Golgi apparatus, which indicates that both domain constructs competed with dynamin II for intracellular binding sites. The *in vitro* and *in vivo* studies provides compelling evidence that dynamin II is required for the formation of exocytic transport vesicles at the TGN.
3. Targeting of dynamin II to the Golgi apparatus requires both PHD and PRD. Recombinant PHD of dynamin II showed a strong affinity to the total brain lipids and bound to plasma membrane and Golgi membranes. EGFP-tagged PHD expressed in HeLa cells indicated a preference for plasma membrane and perinuclear localization. As a new aspect, lipid binding of the recombinant PRD was observed. The specificity of interaction between PRD and membranes is obviously mediated by SH3 domain-containing proteins like amphiphysin I and II as well as syndapin II. We suggest that targeting of cytosolic dynamin II to the membrane sites is specified by the C-terminal PRD, whereas the PHD promotes membrane binding by interacting with membrane lipids.

==========

4. The mechanism(s) by which dynamin II promotes vesicle formation was studied by analysis of binding proteins. Amphiphysin I, syndapin I and II, α- and β-adaptin, and endophilin were bound to PRD of dynamin II, which had been reported also for dynamin I. In addition, γ-adaptin, a component of the adaptor protein complex 1 (AP-1), p47A (AP-3), EEA1 (early endosome-associated protein) and β-tubulin were identified to bind to the PRD. *In vitro* binding to adaptins of AP-1, AP-2 and AP-3, as well as the colocalization of these proteins with endogenous dynamin II in mammalian cells, suggest a function of dynamin II in the formation of large protein complexes which promote the formation of vesicles involved in different intracellular transport pathways.

==========